博士論文

The role of DPPC
in the inflammatory response of macrophages

（生体マクロファージにおける **DPPC** の機能解析）

大木　悠佑

TABLE OF CONTENTS

Introduction **2**

Results **4**

Discussion **12**

Figures and Tables **15**

Materials and methods **47**

References **57**

Acknowledgments **65**

Introduction

Phospholipids, a major component of cell membranes, are composed of hydrophilic polar heads containing polar groups and two hydrophobic fatty acids. The polar head has various polar groups such as choline, serine, ethanolamine, and inositol. The fatty acids are various in terms of the number of carbons and unsaturated bonds[1]. Depending on the combination of the polar group and the two fatty acids, there are more than 1000 different phospholipid species in the body[1]. It is known that the membrane environment formed by these phospholipids affects various cellular functions such as regulation of membrane protein activity[2,3], vesicular transport[3,4], and intracellular signal transduction via lipid microdomains[5,6], and that an appropriate membrane lipid environment is important for cellular functions. On the other hand, the composition of membrane phospholipids varies greatly among tissues and cell types[7], and the subcellular localization of each phospholipid species also varies[8]. Therefore, cells may develop an appropriate membrane lipid environment according to their own functions, but this point remains largely unknown.

Recently, the development of mass spectrometry techniques has enabled the complete analysis of lipid molecular species, and lipidomic analysis of various tissues and cells has been performed. As a result, it has become clear that certain phospholipid species play an important role in the function of specific tissues and cells. For example, phospholipids containing docosahexaenoic acid (DHA), which are abundant in the retina, play an important role in the formation of disc structures in photoreceptors. Mice deficient in lysophosphatidic acid acyltransferase 3 (LPAAT3), the enzyme that introduces DHA into lysophospholipids, have been reported to have impaired vision[9]. However, it remains

unclear what other cell-specific phospholipid species exist and how they relate to cellular functions.

In this study, I found that di-palmitoyl phosphatidylcholine (DPPC), which has only saturated fatty acid palmitate in its fatty acyl chains, is abundant in macrophages in vivo by phospholipid lipidomic analysis using LC-MS/MS. I also found that the introduction of DPPC into macrophages markedly enhanced the production of pro-inflammatory cytokines in response to lipopolysaccharide (LPS) stimulation, a ligand for Toll-like receptor 4 (TLR4). Furthermore, metabolic flux analysis using stable isotopes revealed that DPPC is synthesized by the phospholipid remodeling pathway in macrophages, and the screen for the phospholipid remodeling enzymes involved in DPPC synthesis revealed that lysophosphatidylglycerol acyltransferase 1 (LPGAT1) and lysophosphatidylethanolamine acyltransferase 2 (LPEAT2) are responsible for DPPC synthetic activity in macrophages, in addition to lysophosphatidylcholine acyltransferase 1 (LPCAT1). However, the deletion of LPGAT1 or LPEAT2 in LPCAT1-deficient mice did not further reduce the amount of DPPC in macrophages. To reduce the level of DPPC in macrophages, we searched for lipids that inhibit DPPC synthesis and found that the addition of stearic acid-containing lysophosphatidylcholine (LPC 18:0) markedly reduced DPPC level, resulting in reduced LPS responsiveness. These results suggest that DPPC, which is abundant in macrophages in vivo, plays an important role in enhancing the inflammatory response of macrophages to sense and eliminate foreign substances more efficiently.

Results

DPPC is abundant in macrophages in vivo

Phospholipid lipidomic analysis using LC-MS/MS was performed on various mouse tissues and cultured cells. As a result, it was found that DPPC was more abundant in the PC species of peritoneal macrophages than in the liver and small intestine (Fig. 1). I also compared the amount of DPPC in adipose tissue macrophages and bone marrow-derived macrophages (BMDMs). The amount of DPPC was lower in BMDMs than in peritoneal macrophages or adipose tissue macrophages (Fig. 2). Therefore, we decided to introduce DPPC into these BMDMs and examine how they affect macrophage function.

DPPC promotes LPS responsiveness

It is very difficult to introduce water-insoluble phospholipids into cells[10]. In our laboratory, we have established a system to introduce phospholipids without changing other lipids by adding a mixture of methyl alpha-cyclodextrin (M α CD) and phospholipid liposomes (Fig. 3A). Using this method, DPPC was efficiently introduced into BMDMs, and the amount of DPPC was brought to the same level as that of peritoneal macrophages (Fig.3 B). When these cells were stimulated with LPS, a ligand for TLR4, the amount of pro-inflammatory cytokines released by the DPPC-introduced BMDMs was markedly increased (Fig. 4). Furthermore, the amount of inflammatory cytokines released was also increased when DPPC was introduced into the peritoneal macrophages. (Fig. 5). These results suggest that exogenously-added DPPC promotes macrophage responsiveness to LPS stimulation.

Dipalmitoyl phospholipids are selectively abundant in PC of macrophages in vivo

To examine the role of DPPC abundant in tissue/peritoneal macrophages in the responsiveness to LPS, I tried to identify enzymes responsible for DPPC synthesis in macrophages. I first performed phospholipid metabolism analysis in macrophages to elucidate how the DPPC-rich membrane environment is formed.

Phospholipids are biosynthesized by a *de novo* synthetic pathway (Kennedy pathway)[11,12] and a fatty acid remodeling pathway (Land's cycle)[13]. In the *de novo* synthesis pathway, fatty acids are introduced into glycerol-3-phosphate to form lysophosphatidic acid (LPA), and further fatty acids are introduced to synthesize phosphatidic acid (PA). In general, saturated fatty acids are attached to the *sn*-1 position, and unsaturated fatty acids are attached to the *sn*-2 position[14]. PA is then converted to diacylglycerol (DAG), which is used for the synthesis of PC, phosphatidylethanolamine (PE), and phosphatidylserine (PS) PA is also converted to either CDP-diacylglycerol (CDP-DAG)), which is used for the synthesis of phosphatidylinositol (PI) and phosphatidylglycerol (PG). On the other hand, fatty acids of *de novo* synthesized phospholipids are cleaved by phospholipase A (PLA), and new fatty acids are introduced by lysophospholipid acyltransferase (LPLAT). This process is referred to as the fatty acid remodeling pathway[15,16]. Thus, the fatty acid composition of phospholipids is specified in both the de novo pathway and the fatty acid remodeling pathway (Fig. 6). To elucidate which pathway contributes to DPPC synthesis, we analyzed the molecular species of DAG, PC, PE, and PS in peritoneal macrophages. While DPPC is the major molecular species of PC, dipalmitoyl DAG was not a major molecular species (Fig. 7A), and dipalmitoyl PE (DPPE) and dipalmitoyl PS (DPPS) was hardly detected (Fig. 7C, D). If macrophages synthesize DPPC by de novo pathway, DPPE and DPPS should also be abundant because they are synthesized from dipalmitoyl DAG as well as DPPC. However,

the fact that dipalmitoyl species was unique to PC (Fig. 7B) suggests that DPPC is synthesized by replacing the fatty acid of newly synthesized PC with palmitic acid through the remodeling pathway.

Exogenous palmitic acid is selectively incorporated into PC

Next, stable isotope-labeled palmitic acid (d31-16:0) was added to peritoneal macrophages, and phospholipids were analyzed over time to evaluate the ability to synthesize palmitic acid-containing phospholipids. The added d31-16:0 is incorporated into phospholipids in the de novo pathway or remodeling pathway (Fig. 8A), and phospholipids with one or two d31-16:0 are synthesized (Fig. 8B). These phospholipids with d31-16:0 are distinguished from endogenous phospholipid species by a 31 or 62 shift in mass value. The synthesis of DPPC with one d31-16:0 (d31-DPPC) was remarkable. On the other hand, the synthesis of d31-DPPS and d31-DPPG was not observed. d31-DPPA, d31-DPPE, and d31-DPPI were also synthesized, but at a very low level, less than 2% of d31-DPPC (Fig. 9A). Phospholipids with two d31-16:0 (d62-DPPX) were also analyzed. The synthesis of d62-DPPC was also remarkable (Fig. 9B). These results suggest that the added exogenous palmitic acid is selectively incorporated into PC, which results in the synthesis of DPPC.

Exogenous palmitic acid is incorporated into PC by the remodeling pathway

Although the added palmitic acid is selectively incorporated into PC, it is not possible to distinguish whether it is incorporated by the de novo pathway or the remodeling pathway (Fig. 10). Therefore, I examined the incorporation of d31-16:0 into PC when the de novo synthesis of PC was inhibited.

The introduction of CDP-choline-derived choline into DAG is the final step in the conversion of DAG to PC. Cholinephosphotransferase 1 (CPT1) and choline/ethanolaminephosphotransferase 1 (CEPT1) are responsible for this reaction[17-19] (Fig. 11A). Therefore, I used lentivirus to express shRNA in macrophages to suppress CPT1 and CEPT1 expression. The expression of CPT1 and CEPT1 mRNA was repressed by lentivirus infection (Fig. 11B). *De novo* synthesis of PC can be evaluated by adding stable isotope-labeled choline (d9-choline) and measuring the incorporation of d9-choline into PC[20] (Fig. 11C). CPT1 and CEPT1 double-knockdown (DKD) macrophages were treated with d9-choline. The synthesis of labeled PC was significantly attenuated by CPT1 and CEPT1 DKD (Fig. 11D). Then I examined the incorporation of d31-16:0 into PC in CPT1 and CEPT1 DKD macrophages over time. There was no change in the synthesis of either d31-DPPC (Fig. 12A) or d62-DPPC (Fig. 12B). These results suggest that the exogenous palmitic acid is selectively incorporated into PC by the remodeling pathway rather than the de *novo* pathway.

DPPC and its synthetic activities remain in LPCAT1 KO macrophages

Based on the results of phospholipid metabolism analyses, I focused on LPLATs as a DPPC-producing enzyme in macrophages. Ten genes belonging to the AGPAT family and 4 genes belonging to the MBOAT family are known to be involved in the remodeling pathway[21,22] (Fig. 13). Among them, I focused on LPCAT1, a member of the AGPAT family, which has been reported to exhibit high activity for the synthesis of DPPC, preferring saturated fatty acids as substrates[23]. DPPC is a major lipid component of lung surfactant[24,25], and in LPCAT1 KO mice, lung DPPC is decreased, and lung function is impaired[26,27]. These results suggest that LPCAT1 is also responsible for DPPC synthesis

in macrophages. In fact, macrophages isolated from LPCAT1 KO mice showed reduced DPPC levels, but DPPC was still present at high levels (Fig. 14A). Furthermore, when these macrophages were stimulated with LPS, the inflammatory response was comparable to that of WT macrophages (Fig. 14B). Therefore, I hypothesized that LPLATs other than LPCAT1 might contribute to DPPC synthesis.

Lysophospholipids take two states where its fatty acyl chain is attached to *sn*-1 or *sn*-2 position, and *sn*-2-type lysophospholipids tend to be converted to *sn*-1-type[28]. In our laboratory, we have succeeded in stably storing *sn*-2-type lysophospholipids and measuring the activity of fatty acid incorporation into the *sn*-1 position[28,29]. We have also found that LPCAT1 can introduce fatty acids at either the *sn*-1 or *sn*-2 position[29]. Therefore, I tested whether DPPC synthetic activity remained in LPCAT1 KO macrophages. A membrane fraction from macrophage lysate was mixed with stable isotope-labeled LPC (*sn*-1-d31-acyl LPC or *sn*-2-d31-acyl LPC) and stable isotope-labeled palmitoyl CoA ($^{13}C_{16}$-palmitoyl CoA), and the synthesized DPPC was measured (Fig. 15A). The results showed that activity remained in LPCAT1 KO compared to WT when both LPCs were used (Fig. 15B). In conclusion, DPPC was not reduced enough to affect LPS responsiveness in LPCAT1 KO macrophages, suggesting the presence of other LPLATs involved in DPPC production.

LPGAT1 and LPEAT2 are responsible for DPPC synthesis activity

Therefore, I explored for LPLATs responsible for DPPC production other than LPCAT1. I first established LPCAT1 KO HEK293T cells to eliminate the effect of endogenous LPCAT1 (Fig. 16A). We confirmed that DPPC synthetic activity of LPCAT KO cells was reduced compared to the parental cells (Fig. 16B). The cells were then

overexpressed with LPLATs tagged with FLAG at the N-terminus, and DPPC synthetic activity was measured. The expression of each protein was confirmed by WB (Fig. 17A). Measurement of DPPC synthetic activity showed that LPGAT1 and LPEAT2 had a DPPC synthetic activity (Fig. 17B). LPGAT1 and LPEAT2 were recently found to be LPLATs with fatty acid transfer activity toward *sn*-2 lysophospholipid in our laboratory. In fact, LPCAT1 had the highest activity toward *sn*-1 lysoPC, while LPGAT1 and LPEAT2 had the lower activity compared with LPCAT1. On the other hand, the activity toward the *sn*-2 lysoPC is comparable to that of LPCAT1 (Fig. 17B). Since LPGAT1 and LPEAT2 were found to have DPPC synthetic activity, we examined the effect of suppressing LPGAT1 and LPEAT2 expression on DPPC synthetic activity in LPCAT1 KO macrophages. qPCR confirmed that both LPGAT1 and LPEAT2 mRNA were suppressed (Fig. 18A). In these macrophages, DPPC synthetic activity was markedly reduced (Fig. 18B). These results suggest that LPGAT1 and LPEAT2 are also responsible for DPPC synthesis activity in macrophages *in vivo*.

DPPC is not reduced in LPCAT1/LPGAT1 DKO and LPCAT1/LPEAT2 DKO macrophages

Next, I generated DKO mice by crossing LPCAT1 KO mice with LPGAT1 KO mice and LPEAT2 KO mice, respectively. LPCAT1/LPGAT1 DKO and LPCAT1/LPEAT2 DKO macrophages showed an approximately 80% and 20% reduction in DPPC synthetic activity, respectively (Fig. 19A, B). However, the amounts of DPPC in DKO macrophages were comparable to that of LPCAT1 KO (Fig. 20A, B). In addition, there was no change in the inflammatory response to LPS stimulation between DKO and LPCAT1 single KO macrophages (Fig. 21). These results indicate that although LPGAT1

and LPEAT2 have DPPC synthetic activity, they do not contribute to the level of DPPC in macrophages.

DPPC is significantly reduced by the addition of LPC 18:0

Analysis using d31-16:0 suggests that macrophages synthesize DPPC by incorporating palmitic acid in the remodeling pathway (Fig. 12A, B). Therefore, I investigated whether DPPC synthesis could be inhibited by adding LPC or fatty acids, which are substrates for DPPC synthesis in the remodeling pathway. For example, if a fatty acid other than palmitic acid is added, it competes with palmitic acid in the LPCAT reaction, resulting in inhibition of DPPC synthesis. Likewise, if an LPC whose fatty acid is not palmitic acid is added, it competes with palmitoyl LPC in the LPCAT reaction. Therefore, we added various fatty acids and LPCs to the peritoneal macrophages and searched for lipids that decrease DPPC. For fatty acids I tested stearic acid (18:0), oleic acid (18:1), linoleic acid (18:2), arachidonic acid (20:4), and eicosapentaenoic acid (EPA, 20:5). A decrease in DPPC was observed only with the addition of 18:0 (Fig. 22A). However, PC 34:0, which is expected to have 16:0 and 18:0 as fatty acyl chains, also increased more than the decrease in DPPC (Fig. 22B). PC 34:0 also promoted the inflammatory response by DPPC (data not shown), so it was inappropriate to verify the contribution of DPPC to the inflammatory response in this condition. Next, I examined the effect of LPC 18:0 and LPC 18:1. The addition of LPC 18:0 decreased DPPC, while the addition of LPC 18:1 did not change the amount of DPPC (Fig. 23). The addition of LPC 18:0 increased PC 34:0, but the extent of the increase was small compared to that of the decrease in DPPC. These results indicate that the addition of LPC 18:0 successfully reduced the endogenous DPPC in macrophages.

LPS responsiveness is attenuated by the addition of LPC18:0

I examined the effect of LPC 18:0 on inflammatory responses by stimulating macrophages with LPS. Macrophages treated with LPC 18:0 showed a marked decrease in the amount of pro-inflammatory cytokines released in response to LPS stimulation (Fig. 24). LPCs are known to induce apoptosis when added to cells[30]. It is possible that the change in LPS responsiveness upon addition of LPC 18:0 is not due to a decrease in DPPC but is a property of LPC themselves. To rule out this possibility, we examined LPS responsiveness by adding LPC 18:1, which has no effect on DPPC reduction (Fig. 23). The addition of LPC 18:1 did not attenuate the LPS response (Fig. 25). Furthermore, the expression of TLR4 on the cell surface was analyzed by flow cytometry when LPC was added, and the expression of TLR4 was not decreased by either LPC 18:0 or LPC 18:1 (Fig. 26). Furthermore, the effect of LPC 18:0 on LPS responsiveness was partially restored when DPPC was introduced into macrophages (Fig. 27B). On the other hand, PC 34:1 (POPC), in which one of the two fatty acids is unsaturated, did not restore reduced LPS responsiveness by LPC 18:0. These results strongly suggest that the addition of LPC 18:0 attenuated the LPS responsiveness due to the decrease in DPPC.

Discussion

In the present study, I found that DPPC was abundant in tissue/peritoneal macrophages and had a function to positively regulate inflammatory responses of macrophages.

It has been reported that lipid domains called lipid rafts are important for the activation of TLR4[31-33]. In general, lipid rafts are known to be enriched in lipids such as sphingomyelin and cholesterol[34,35]. On the other hand, saturated phospholipids such as DPPC have also been suggested to be enriched in lipid rafts, and these lipids may promote the formation of lipid rafts[36,37]. It is possible that DPPC promotes lipid raft formation, which in turn promotes inflammatory responses. Interestingly, the enhancement of the inflammatory response by DPPC was also observed when the ligands of TLRs other than TLR4 were used (Fig. 28). It has been reported that lipid rafts on endosomes are important for the activation of TLR9[38]. The phospholipid delivery system established in our laboratory can deliver phospholipids not only to the cell surface but also to intracellular membranes such as endosomes, based on experiments using fluorescent phospholipids. Therefore, it is likely that the introduction of DPPC also enhanced the responsiveness of endosomal TLRs. These results suggest that DPPC plays an important role in the efficient detection and elimination of foreign substances by promoting the activation of not only TLR4 but also other TLRs. On the other hand, LPCAT1 depletion and LPC 18:0 treatment caused similar levels of DPPC reduction in macrophages, but its effects on inflammatory responses were very different. Given that LPC 18:0 significantly attenuated LPS responsiveness, it is likely that DPPC in the plasma membrane was efficiently reduced. This will be verified by measuring DPPC in the cell membrane using an isolation technique of the plasma membrane. It will also be interesting to see if LPC 18:0 affects the responsiveness of endosomal TLRs.

There are many examples of lipid rafts being important in signal transduction other than TLR4, such as Immunoglobulin E mediated signaling[39], T cell receptor[40] and the B cell receptor[41]. It has been reported that the saturated PC-rich membrane environment formed by LPCAT1 in cancer cells is favorable for the survival of cancer cells by enhancing oncogenic receptor signaling such as EGFR[42]. In addition, we have found that DPPC are also abundant in immune cells other than macrophages, such as dendritic cells and B cells (data not shown). These cells have in common the ability to present antigens. These cells take up invading pathogens into their cells, where the antigen proteins are degraded to peptides and then presented to the outside of the cell by MHC II, which is recognized and activated by T cells[43]. Interestingly, it has been reported that MHC II localizes to lipid rafts and forms clusters[44,45] and that lipid rafts are important for efficient antigen presentation[46,47]. Therefore, it is possible that DPPC forms rigid lipid rafts or lipid raft-like domains to enhance the efficiency of antigen presentation by MHC II, as shown in the inflammatory response in the present study.

We found that LPGAT1 and LPEAT2 have DPPC synthetic activity and LPGAT1 significantly contributes to DPPC synthetic activity in macrophages. However, the analysis of LPCAT1/LPGAT1 DKO macrophages showed that LPGAT1 did not contribute to the amount of DPPC in macrophages. However, flux analysis with d31-16:0 showed that DPPC was synthesized by the remodeling pathway, suggesting that yet another LPLAT is responsible for DPPC synthesis. LPCAT2 has an EF-hand motif and is known as a Ca^{2+}-requiring LPLAT[23]. Since there are no Ca^{2+} ions in my experimental system, it is possible that the Ca^{2+}-requiring activities such as LPCAT2 have not been properly evaluated. In fact, when I compared the activity of LPCAT1 with and without Ca^{2+}, I found that the addition of Ca^{2+} enhanced the activity by almost twofold (Fig. 29).

Interestingly, the enhancement of activity was higher in LPCAT1 KO than in WT, suggesting that the Ca^{2+}-requiring activity was increased in LPCAT1 KO macrophages. Besides LPCAT2, only LPCAT1 is a known LPLAT with an EF-hand motifs[48]. By investigating the contribution of these Ca^{2+}-requiring LPLATs to DPPC synthesis, it is hoped that the full picture of the DPPC synthetic pathway in macrophages will be revealed.

In conclusion, I found that DPPC is important for the inflammatory response of macrophages and that the amount of DPPC can be altered by lysoPC. LysoPC is present in blood at concentrations of several hundred μM and can be generated from the cell membrane by the action of PLA_2[49,50]. Further studies focusing on the amount of DPPC in macrophages are expected to advance our understanding of macrophage trait changes in various pathological conditions.

Figure 1

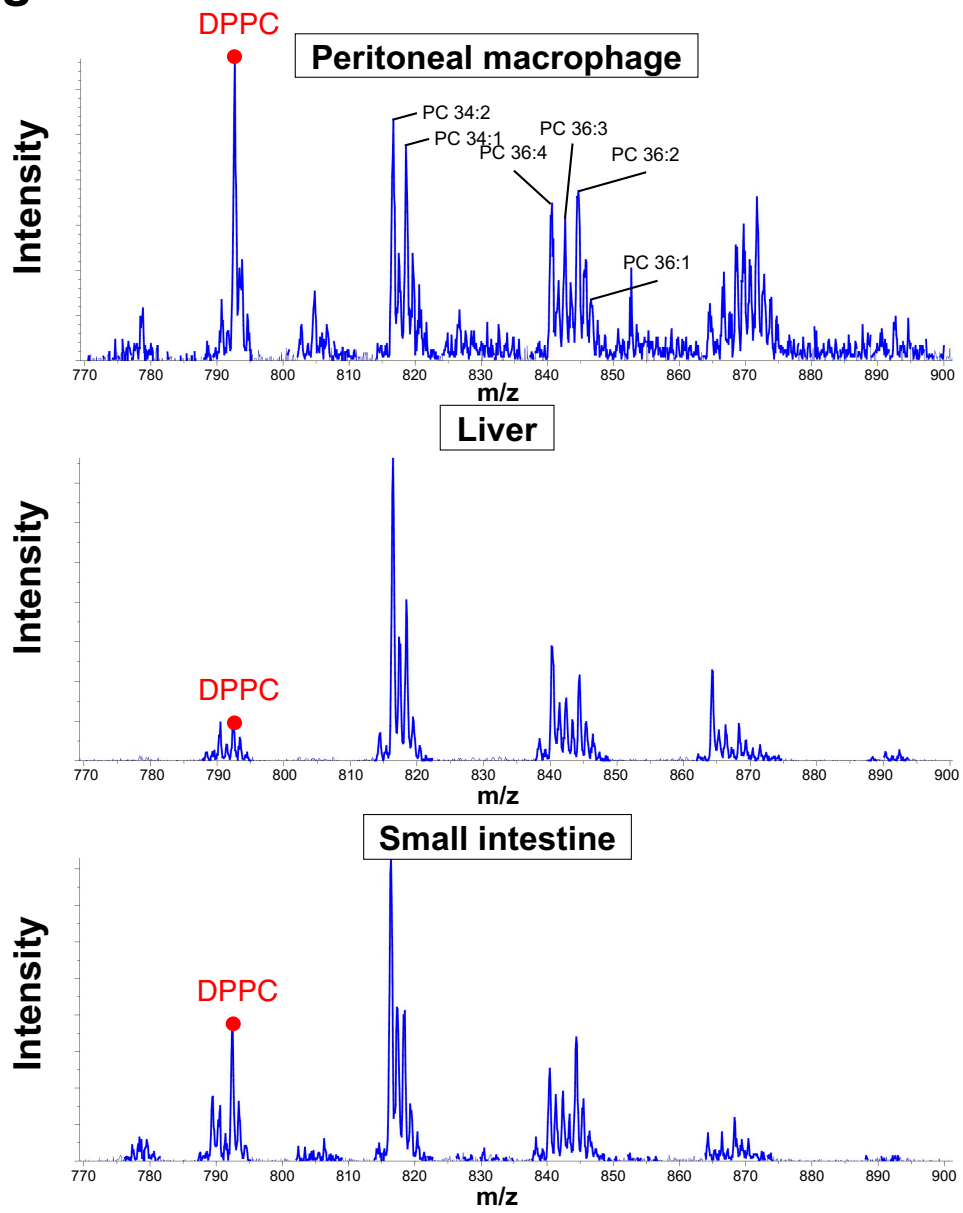

Fig. 1 DPPC are abundant in macrophages in vivo

Mass spectrum of PC of peritoneal macrophages, liver, and small intestine.

Figure 2

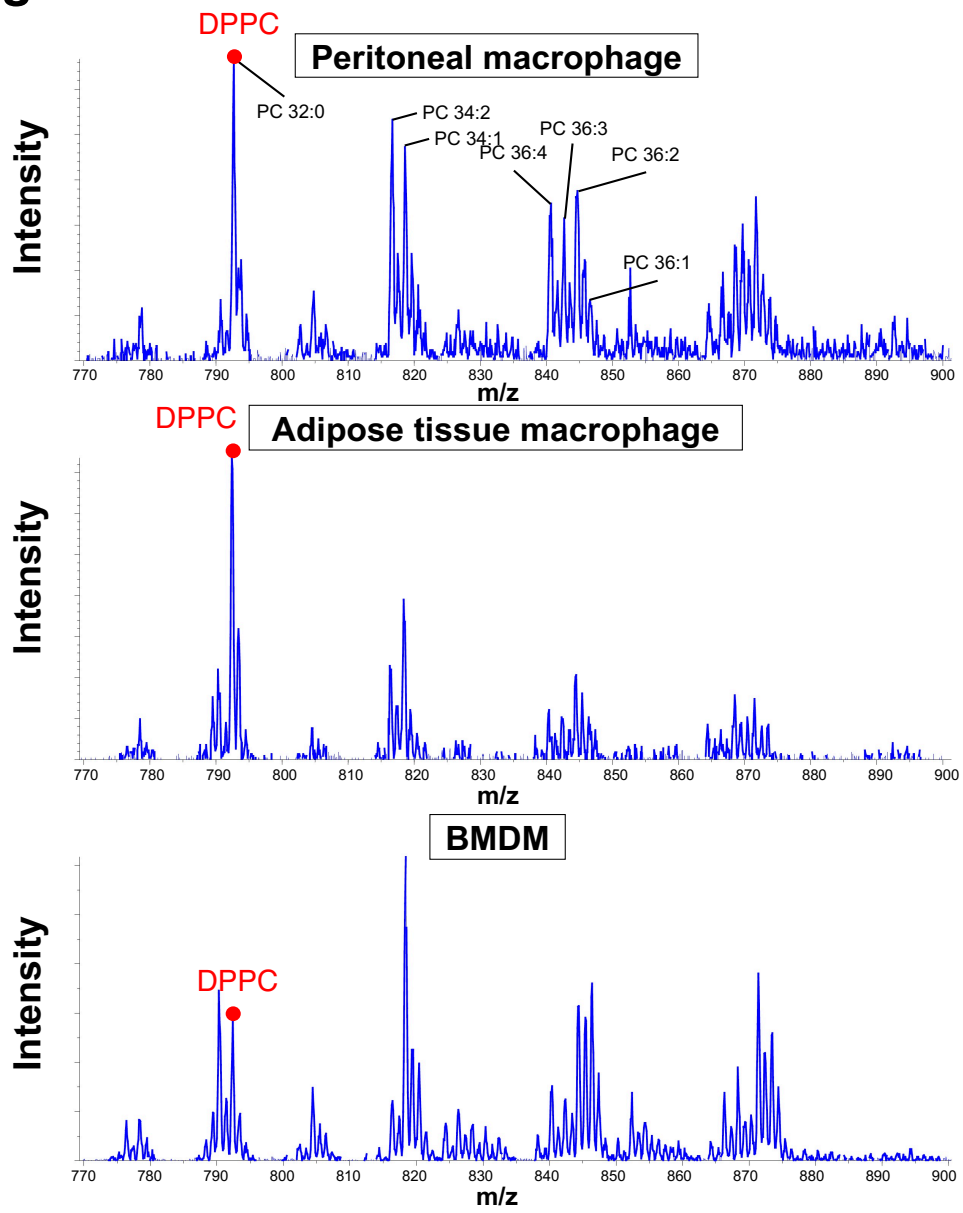

Fig. 2 Fewer DPPCs in BMDMs compared to macrophages in vivo

Mass spectrum of PC of peritoneal macrophages, adipose tissue macrophage, and BMDM.

Figure 3

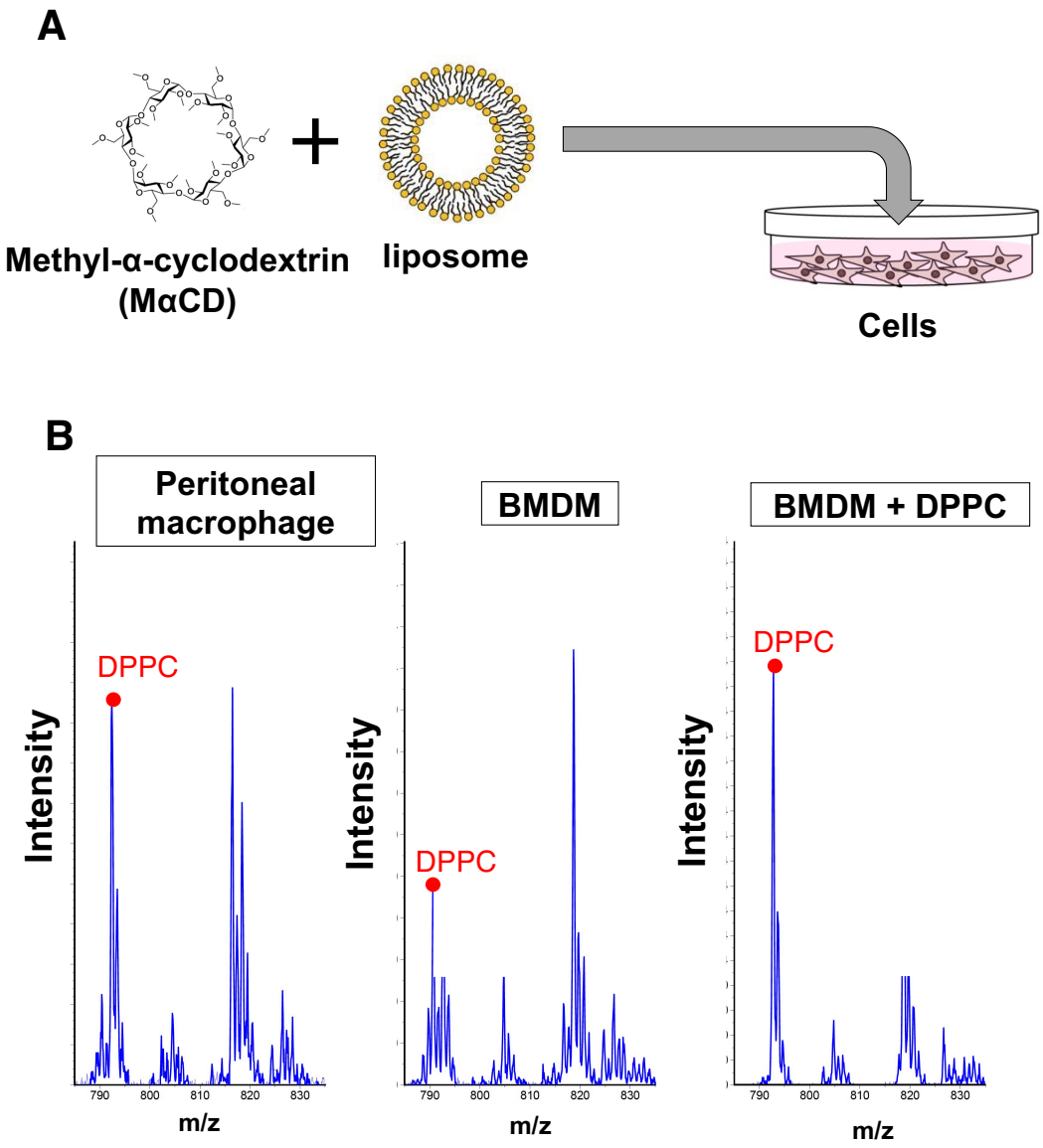

Fig. 3 Introduction of DPPC into BMDM by phospholipid transfer system

(A) Experimental system for phospholipid introduction。

(B) Mass spectrum of PC of peritoneal macrophages and BMDM introduced DPPC.

Figure 4

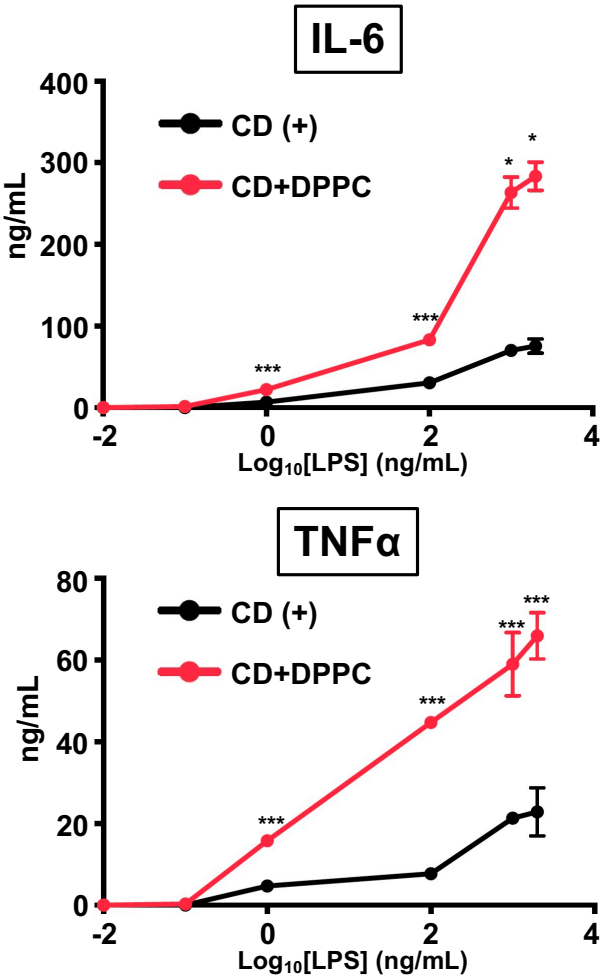

Fig. 4 LPS responsiveness is enhanced in BMDM with DPPC

Cytokine secretion by DPPC-introduced and LPS-stimulated BMDMs. Mean ± SEM. n = 3. *p<0.05, ***p <0.001. Statistical analysis was done by one-way ANOVA with Tukey's test.

Figure 5

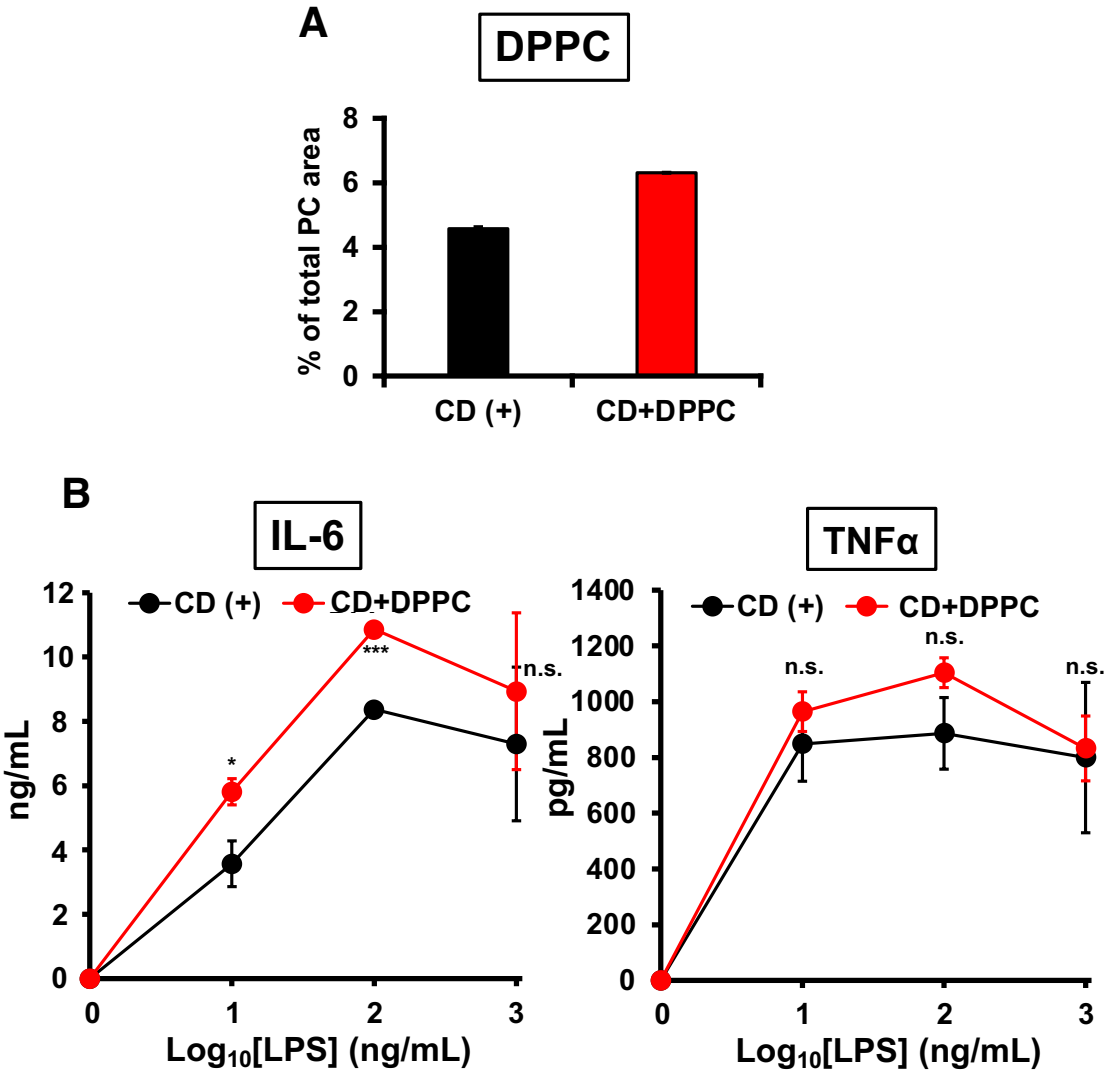

Fig. 5 LPS responsiveness is also enhanced in DPPC-transfected periotneal macrophages

(A) The amount of DPPC in DPPC-introduced peritoneal macrophages was analyzed by LC-MS/MS. Normalized peak area of the total amount and compositions of molecular species are shown. Mean ± SEM. n = 3.

(B) Cytokine secretion by DPPC-introduced and LPS-stimulated peritoneal macrophages. Mean ± SEM. n = 3.

n.s., not significant. *p<0.05, ***p <0.001. Statistical analysis was done by one-way ANOVA with Tukey's test.

Figure 6

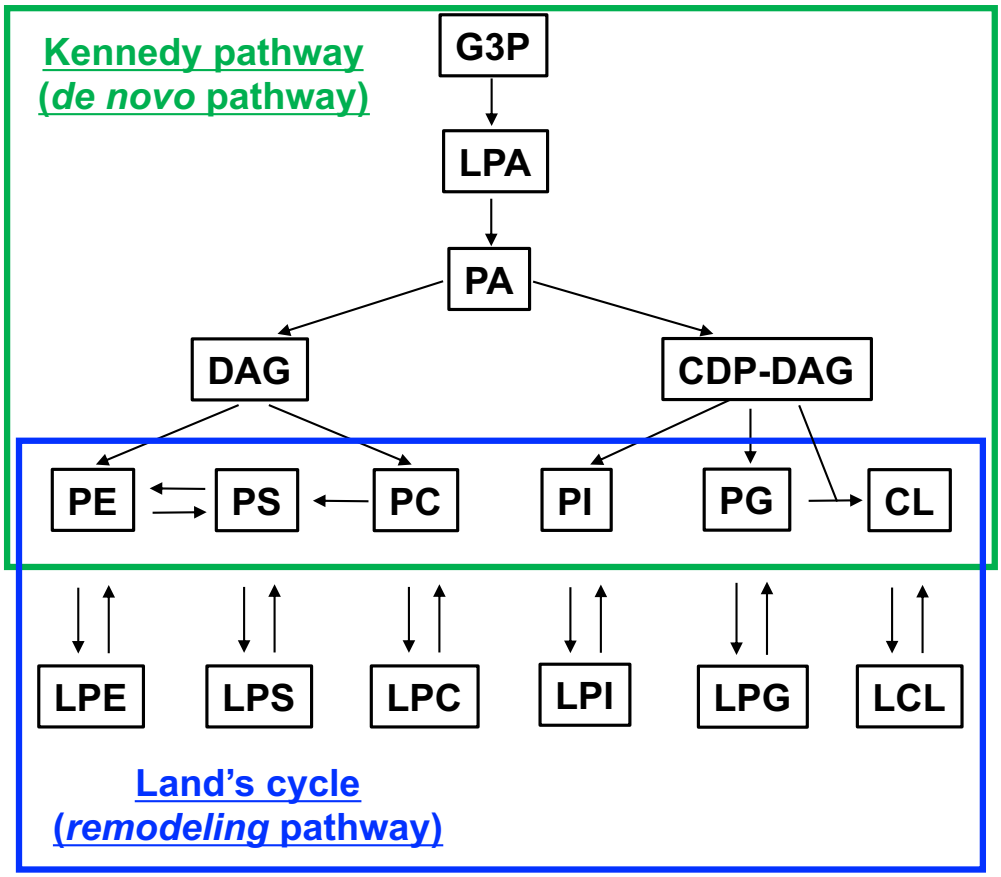

Fig. 6 Pathways of phospholipid biosynthesis

Phospholipids are first synthesized through the de novo pathway (Kennedy pathway) and then modified through the remodeling pathway (Land's cycle). LPC, lyso-PC; LPE, lyso-PE; LPS, lyso-PS; LPI, lyso-PI; LPG, lyso-PG; LCL, lyso-CL.

Figure 7

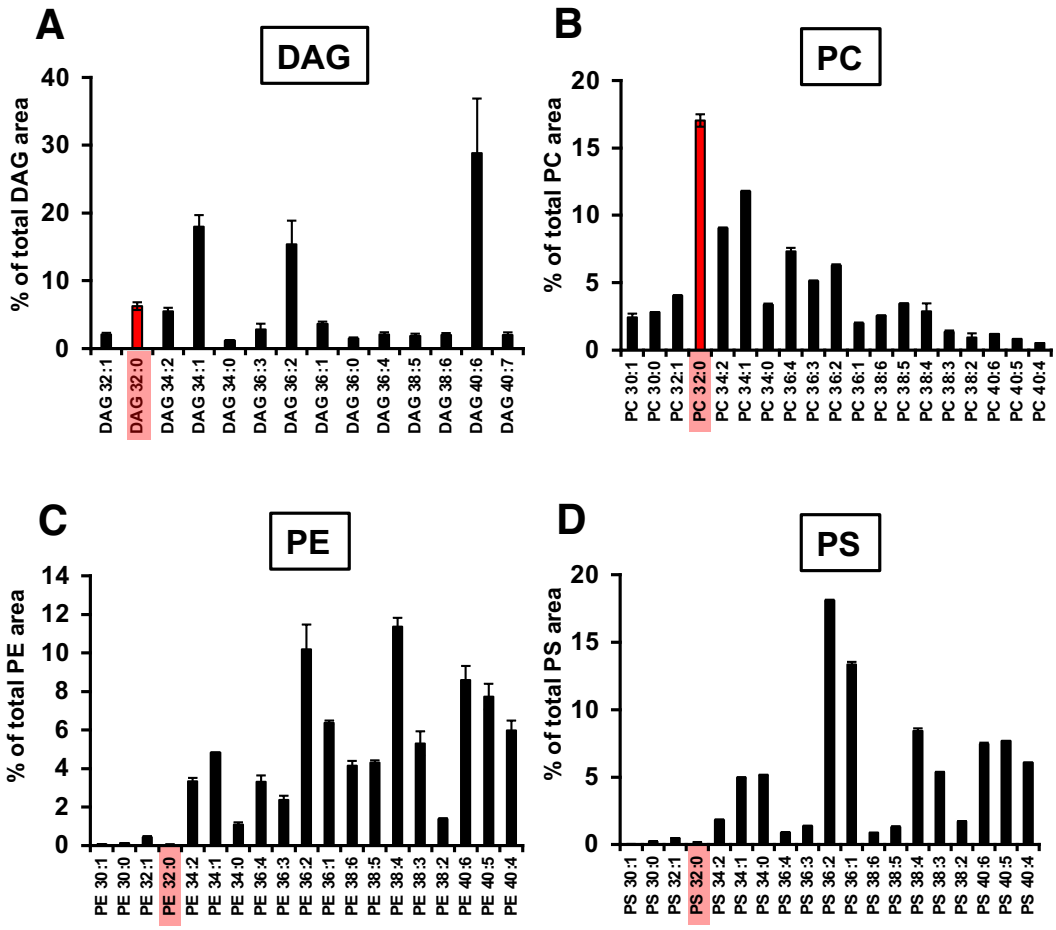

Fig. 7 Dipalmitoyl phospholipids are selectively abundant in PC

(A)-(D) Phospholipids in peritoneal macrophages were analyzed by LC-MS/MS. Normalized peak area of the total amount and compositions of molecular species are shown. n = 3, mean ± SEM.

Figure 8

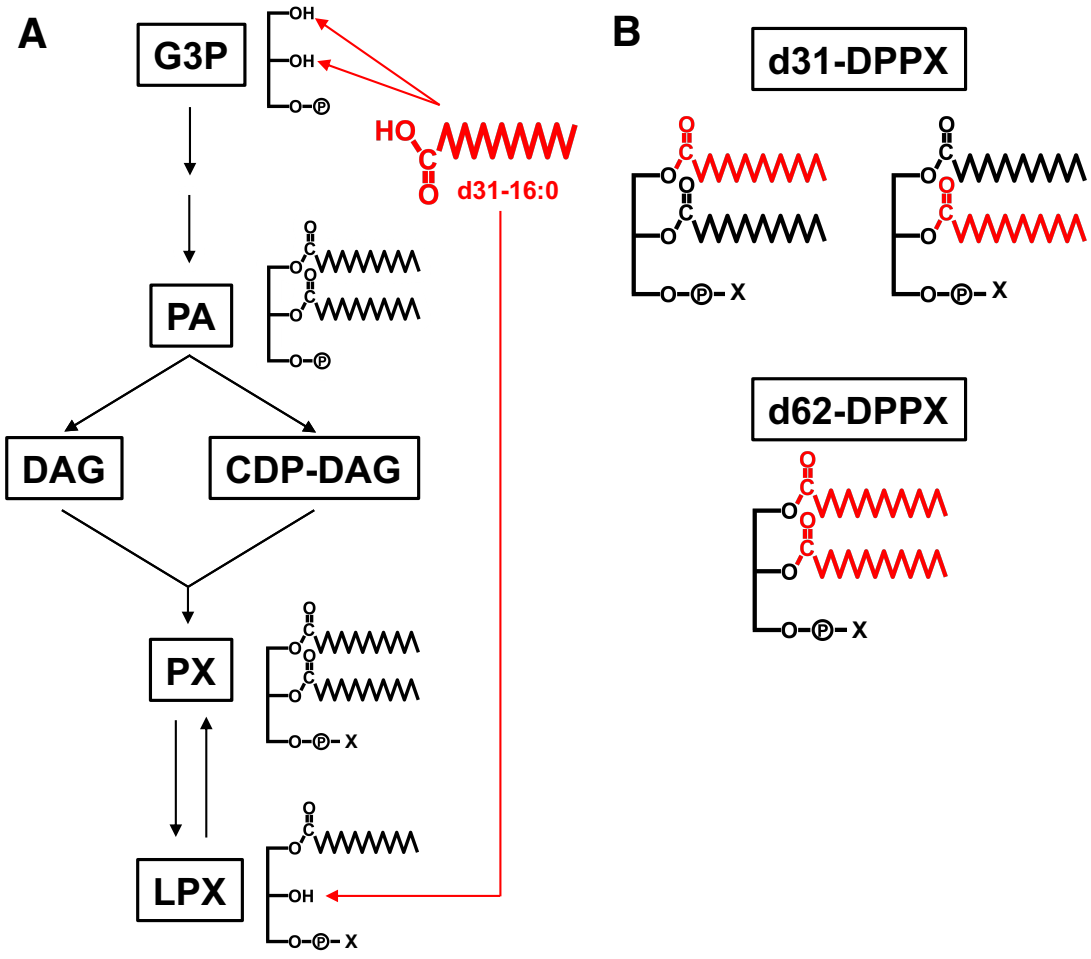

Fig. 8 Evaluation of the ability to synthesize palmitic acid-containing phospholipids using d31-16:0

(A) d31-16:0 is taken by de novo pathway or remodeling pathway.

(B) Phospholipids with one or two d31-16:0.

Figure 9

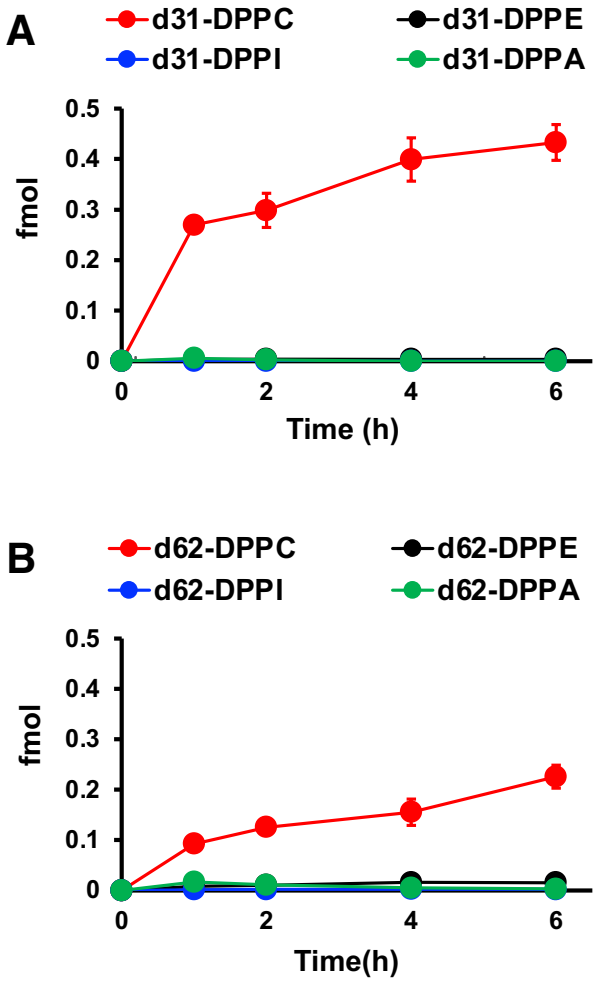

Fig. 9 d31-16:0 is selectively incorporated into PC

(A) The synthesis of phospholipids with one d31-16:0 over time was measured by LC-MC/MC. Absolute quantification was performed from calibration curves for each phospholipid standard. Mean ± SEM. n = 3.

(B) Synthesis of phospholipids with two d31-16:0 over time. Mean ± SEM. n = 3.

Figure 10

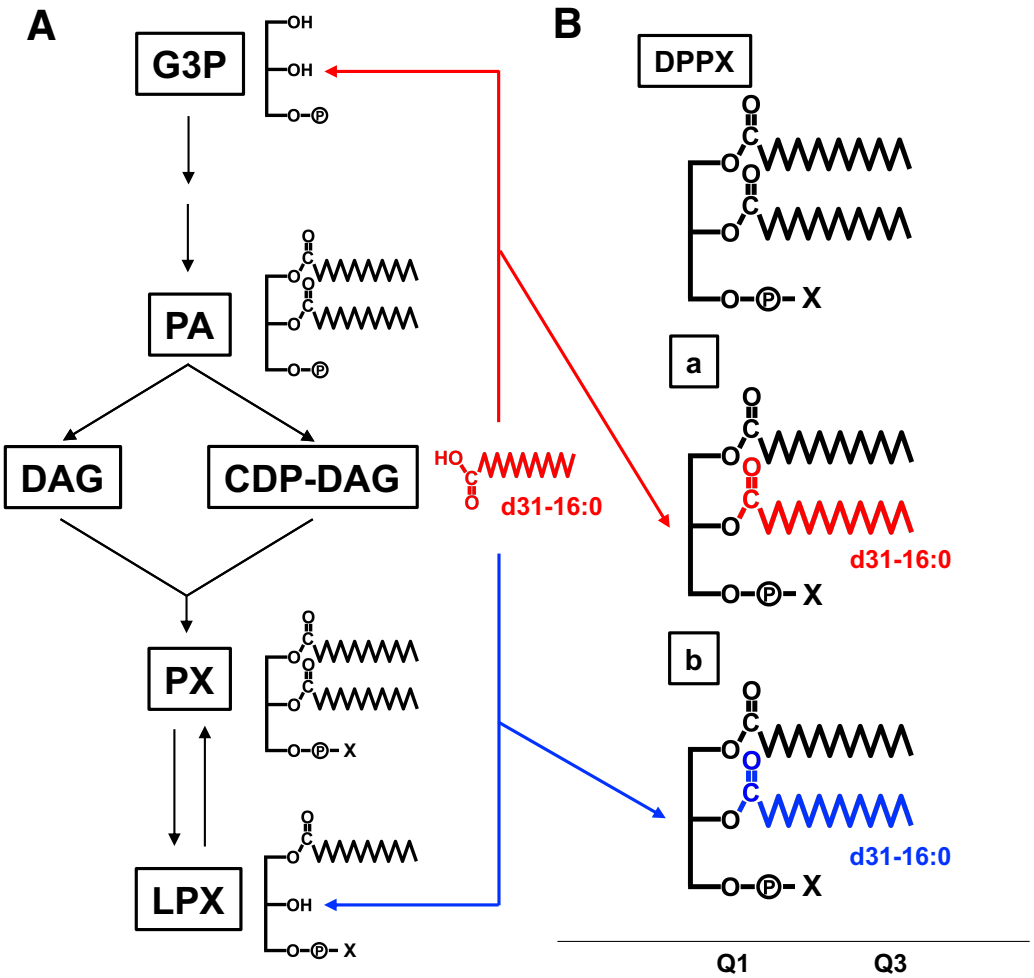

	Q1	Q3
DPPX	X	255
a	X+31	255+31
b	X+31	255+31

Fig. 10 The pathway by which d31-16:0 is taken up cannot be determined by LC-MS
(A) d31-16:0 is taken by de novo pathway or remodeling pathway.
(B) Endogenous dipalmitoyl phospholipids (DPPX) and dipalmitoyl phospholipids incorporating d31-16:0 in the de novo pathway (a) or d31-16:0 in the remodeling pathway (b). The table shows the measured values for Q1 and Q3. The values of (a) and (b) are identical and cannot be distinguished by MS.

Figure 11

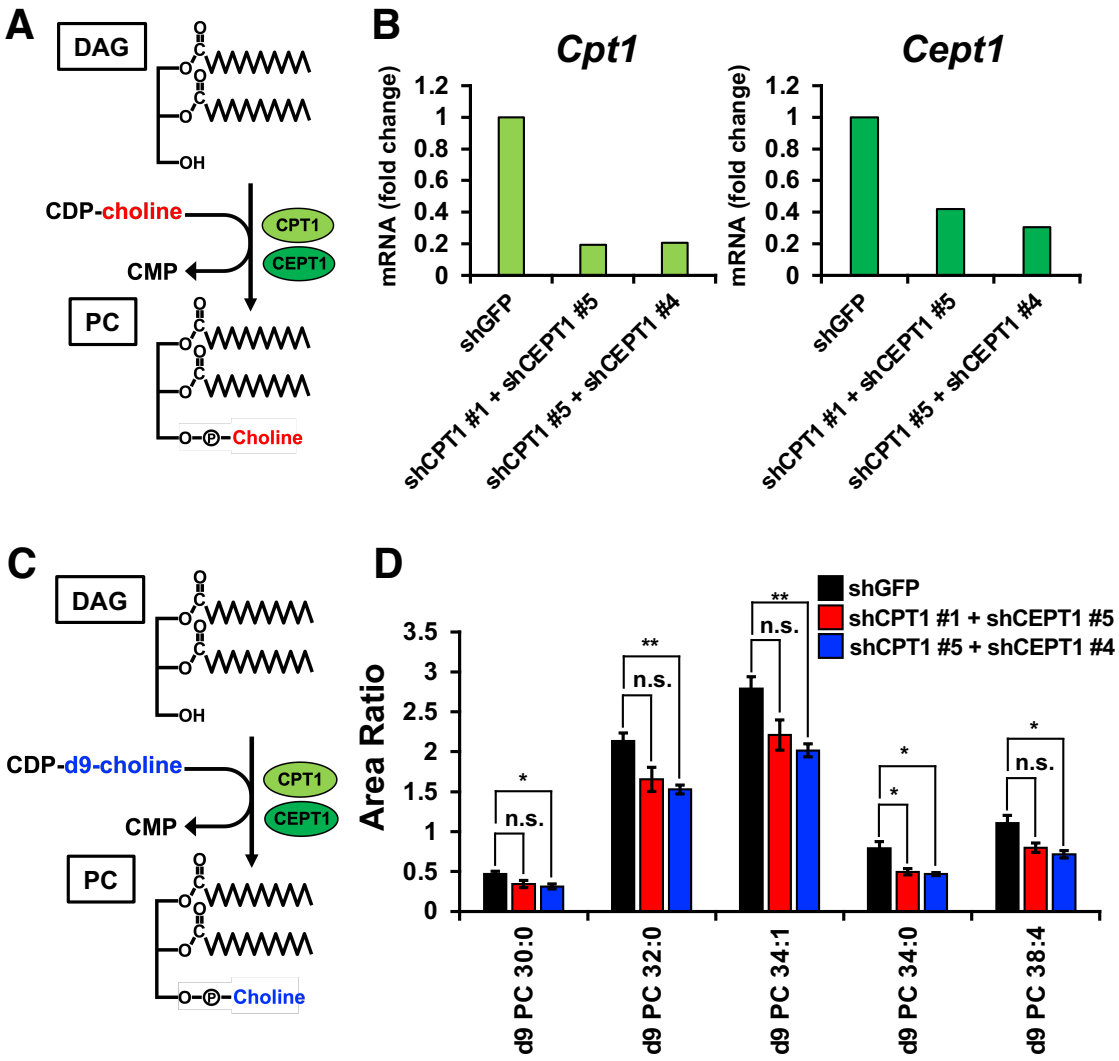

Fig. 11 Inhibition of CPT1 and CEPT1 expression suppresses the de novo synthesis of PC

(A) Synthesis of PC in de novo pathway.

(B) Expression repression efficiency of *Cpt1* and *Cept1* mRNA were analyzed by qRT-PCR and normalized to 18S ribosomal RNA expression.

(C) Evaluation of novel synthesis of PC using d9-choline.

(D) Novel synthesis of PC for Cpt1 and Cept1 expression suppressed macrophages. Mean ± SEM. n = 3. n.s., not significant. *p<0.05, ***p <0.001. Statistical analysis was done by one-way ANOVA with Tukey's test.

Figure 12

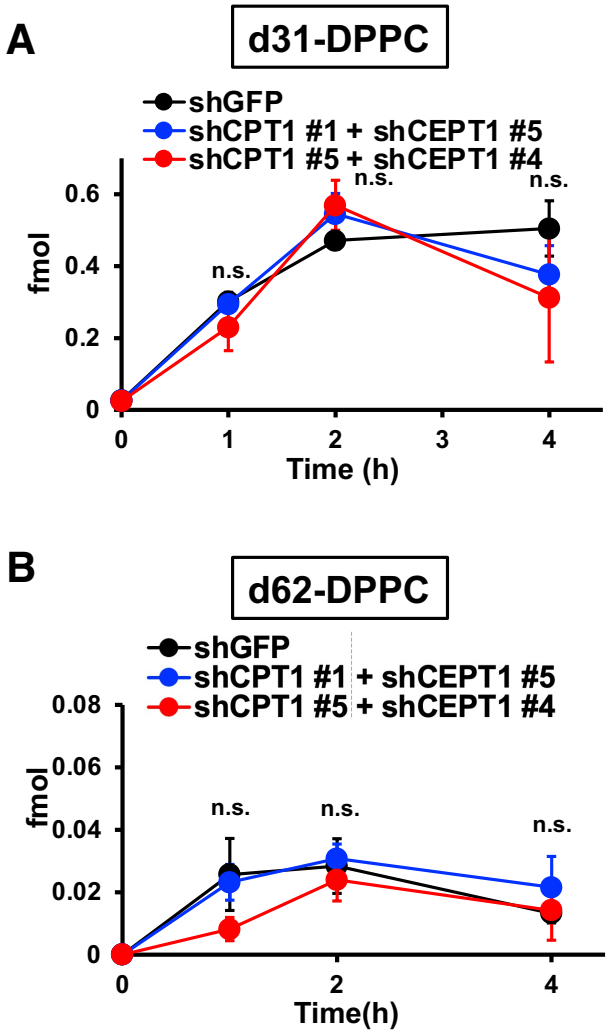

Fig. 12 Inhibition of PC de novo synthesis does not alter the incorporation of d31-16:0 into PC

(A) The synthesis of phospholipids in Cpt1 and Cept1 expression suppressed macrophages with one d31-16:0 over time was measured by LC-MC/MC. Mean ± SEM. n = 3.

(B) Synthesis of phospholipids with two d31-16:0 over time. Mean ± SEM. n = 3. n.s., not significant. Statistical analysis was done by one-way ANOVA with Tukey's test.

Figure 13

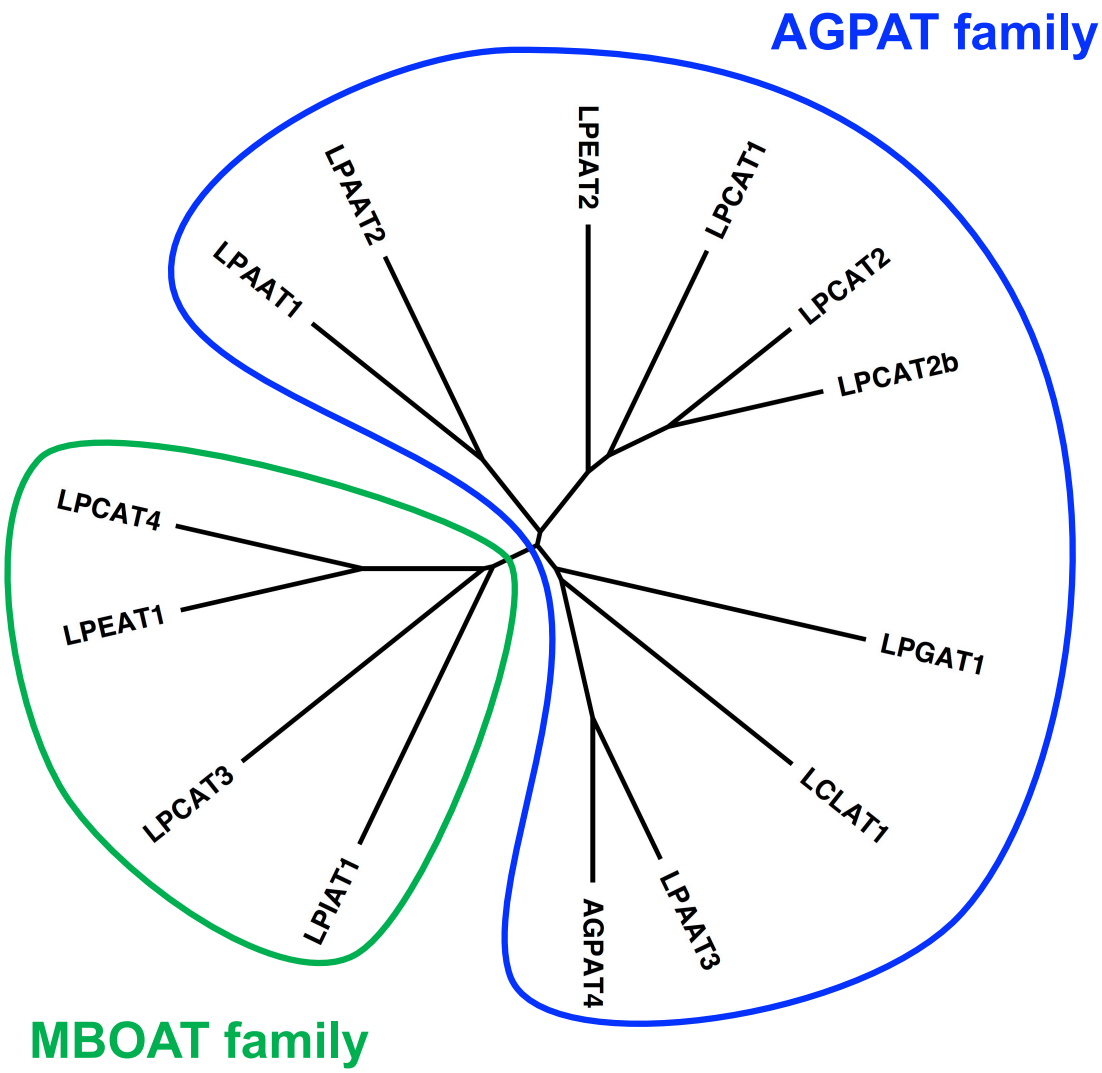

Fig. 13 Phylogenetic tree of the LPLAT family
The phylogenetic tree was analyzed with Clustal Omega and edited with FigTree.

Figure 14

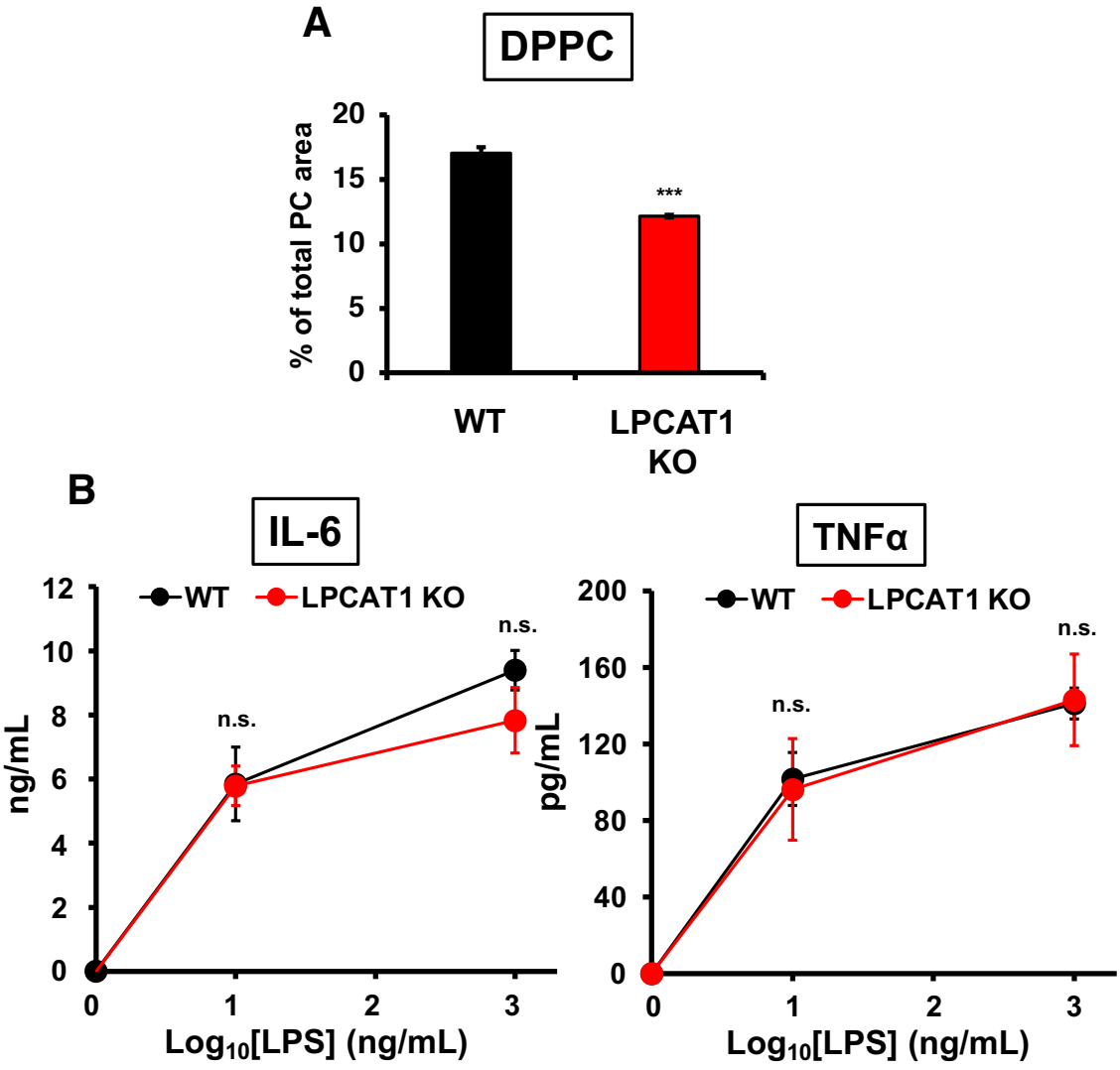

Fig. 14 DPPC remains in LPCAT1 KO macrophages and LPS responsiveness is not altered

(A) The amount of DPPC in LPCAT KO peritoneal macrophages was analyzed by LC-MS/MS. Normalized peak area of the total amount and compositions of molecular species are shown. Mean ± SEM. n = 3.

(B) Cytokine secretion by LPCAT KO LPS-stimulated peritoneal macrophages. Mean ± SEM. n = 3. n.s., not significant. ***p <0.001. Statistical analysis was done by one-way ANOVA with Tukey's test.

Figure 15

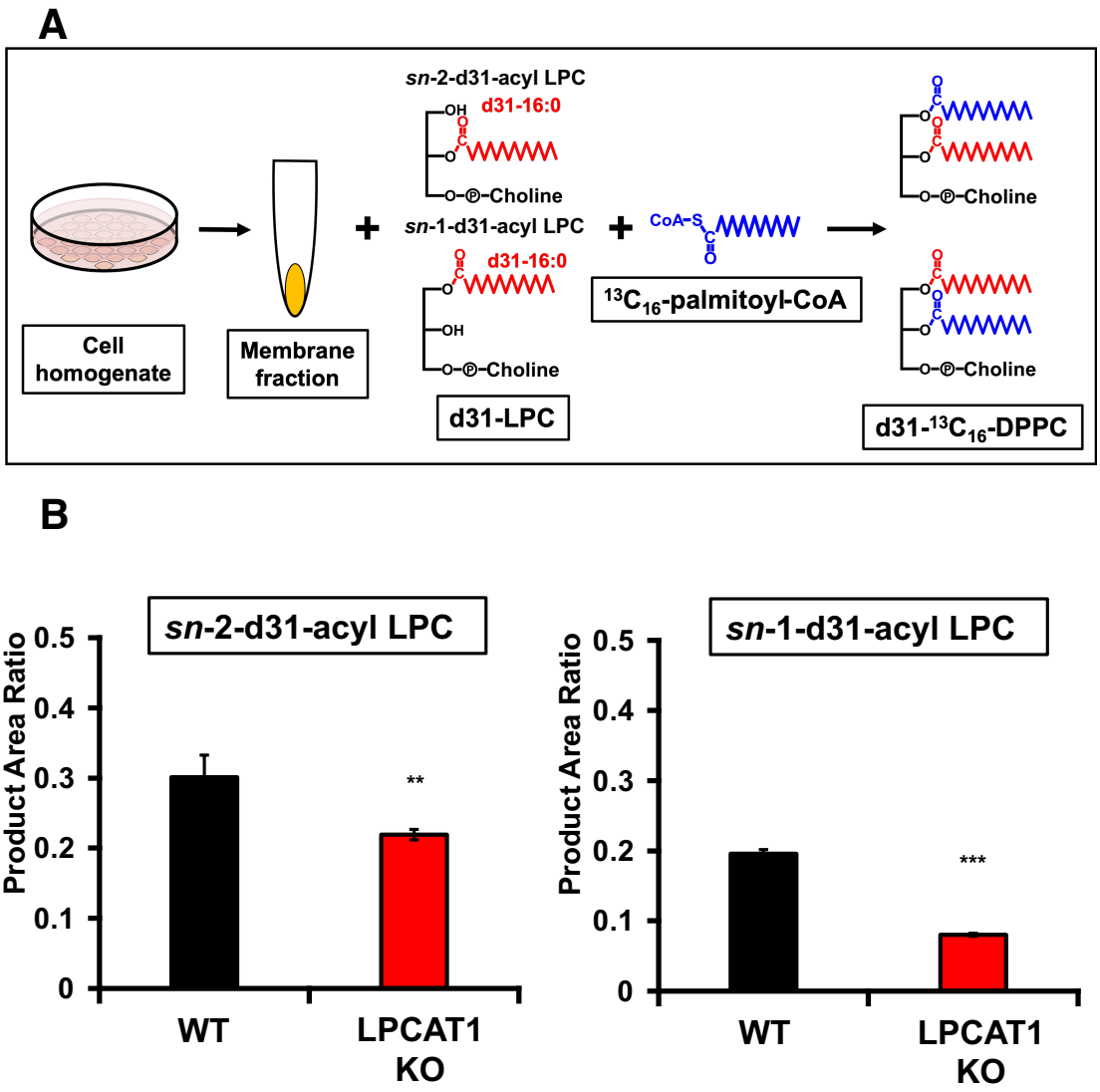

Fig. 15 DPPC synthesis activity remains in LPCAT1 KO macrophages

(A) DPPC synthesis activity measurement method.

(B) DPPC synthesis activity of LPCAT KO macrophages. sn-2-acyl LPC and sn-1-acyl LPC were used to measure the activity of introduction into the *sn*-1 and *sn*-2 positions, respectively. Mean ± SEM. n = 3. **p<0.01, ***p <0.001. Statistical analysis was done by one-way ANOVA with Tukey's test.

Figure 16

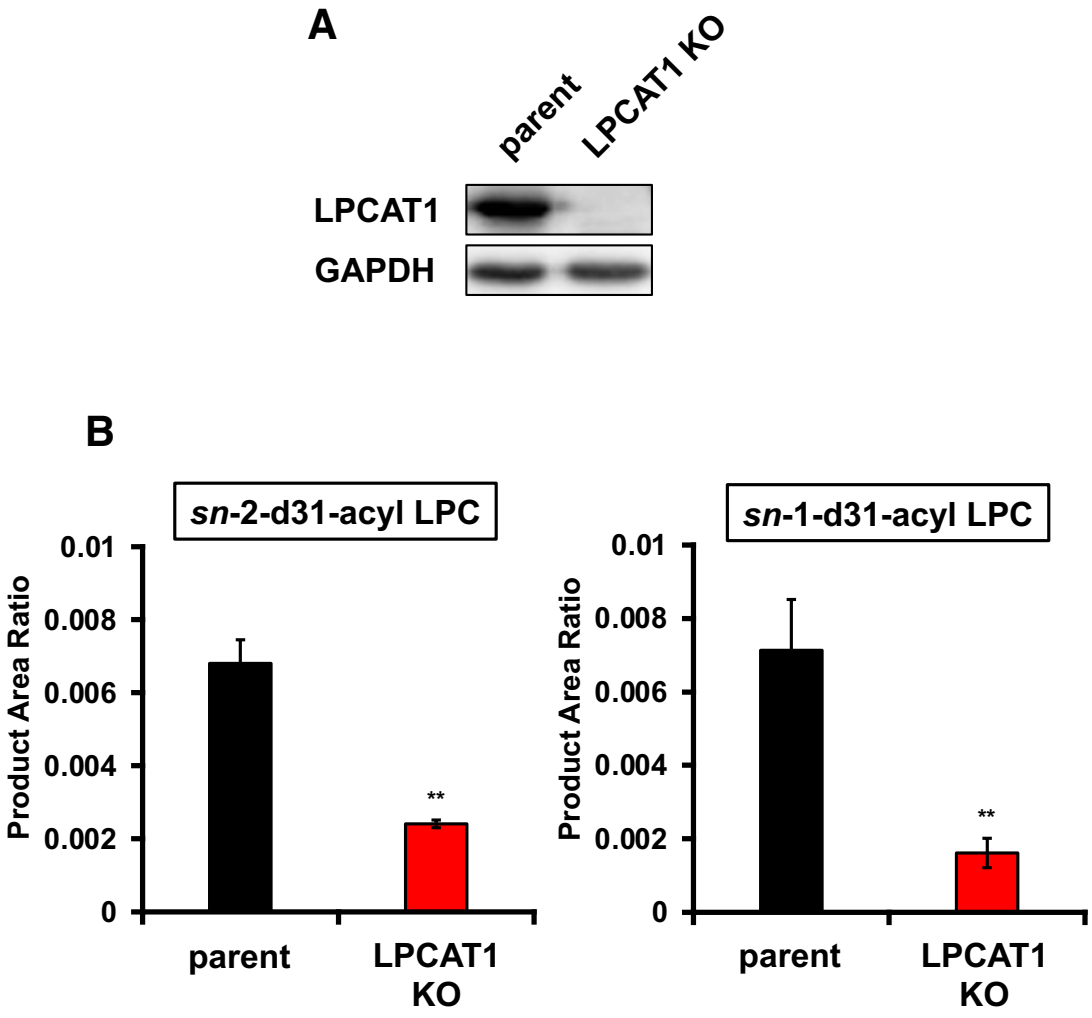

Fig. 16 Establishment of LPCAT1 KO HEK293T cells

(A) Expression analysis of LPCAT1 protein in parental cells and LPCAT1 KO HEK293T cells by western blotting.

(B) DPPC synthesis activity of LPCAT KO HEK293T cells. *sn*-2-d31-acyl LPC and *sn*-1-d31-acyl LPC were used to measure the activity of introduction into the *sn*-1 and *sn*-2 positions, respectively. Mean ± SEM. n = 3. **p<0.01. Statistical analysis was done by one-way ANOVA with Tukey's test.

Figure 17

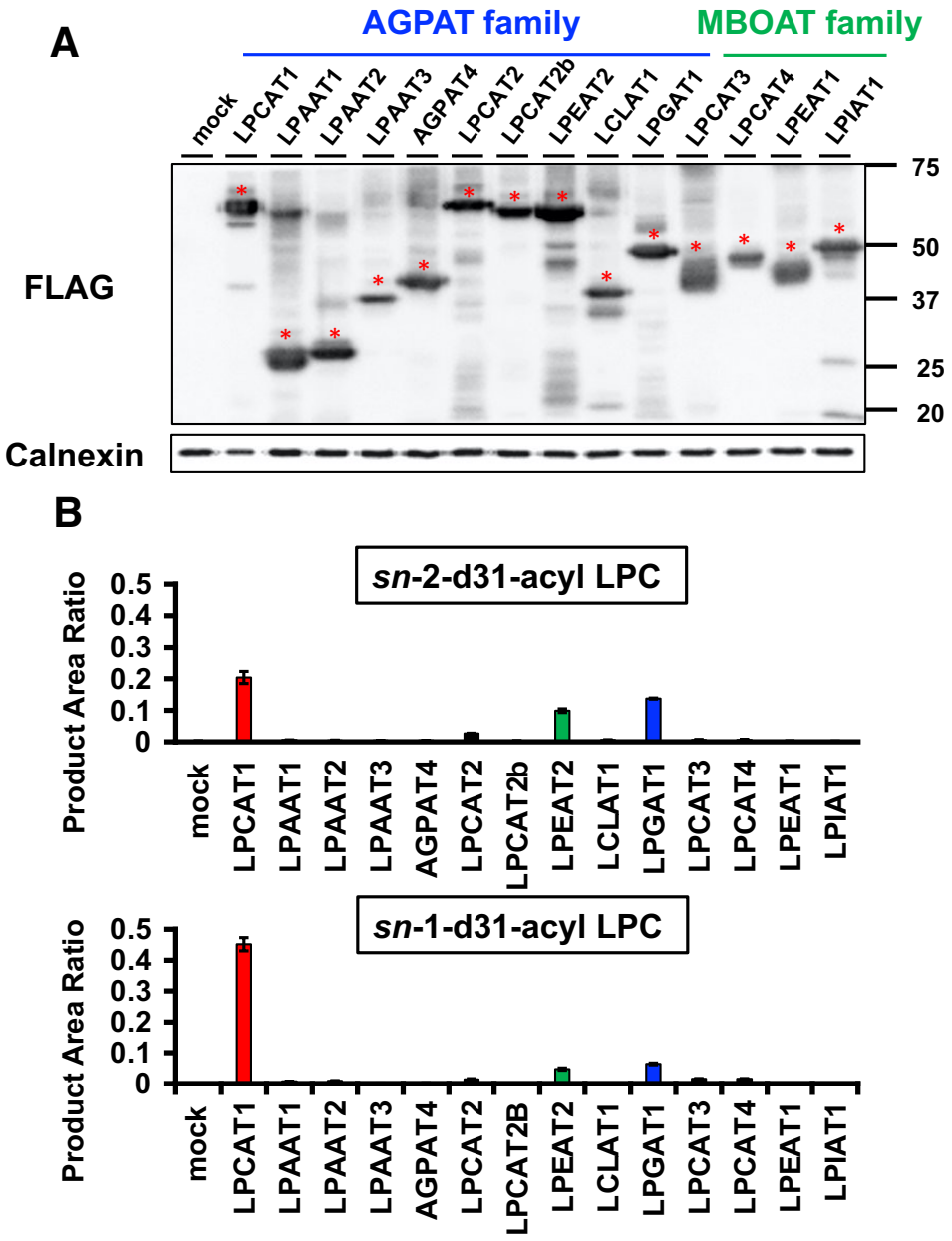

Fig. 17 LPGAT1 and LPEAT2 have DPPC synthesis activity

(A) Protein expression levels in membrane fractions of each LPLAT-overexpressing cell were analyzed by western blotting. Red asterisks indicate predicted bands.

(B) DPPC synthesis activity of LPLAT-overexpressing cells. *sn*-2-d31-acyl LPC and *sn*-1-d31-acyl LPC were used to measure the activity of introduction into the *sn*-1 and *sn*-2 positions, respectively. Mean ± SEM. n = 3. Statistical analysis was done by one-way ANOVA with Tukey's test.

Figure 18

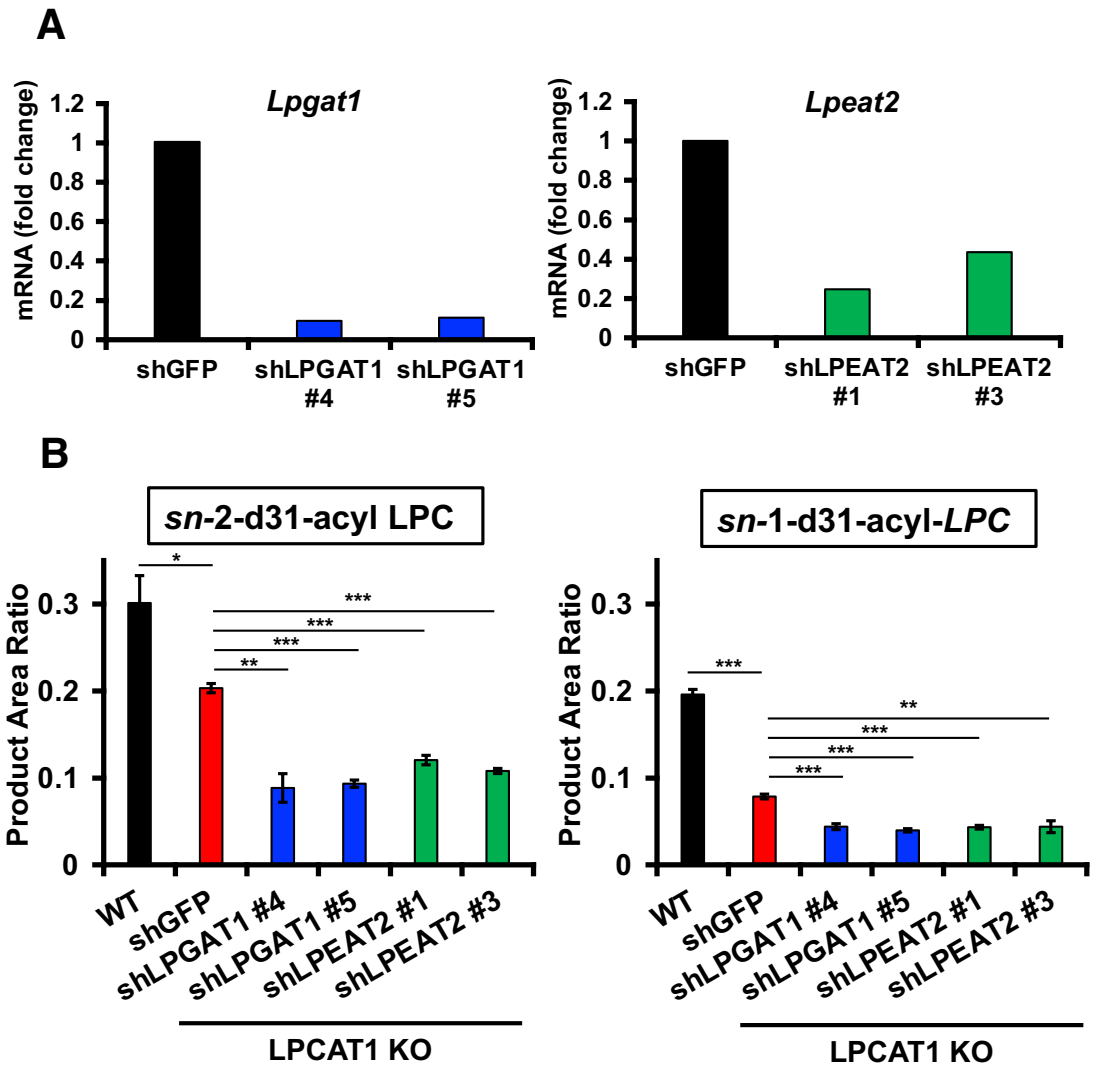

Fig. 18 LPGAT1 and LPEAT2 contribute to DPPC synthesis activity in macrophages in vivo

(A) Expression repression efficiency of *Lpgat1* and *Lpeat2* mRNA were analyzed by qRT-PCR and normalized to 18S ribosomal RNA expression.

(B) DPPC synthesis activity of LPCAT1 KO peritoneal macrophages with suppressed expression of Lpgat1 and Lpeat2. *sn*-2-d31-acyl LPC and *sn*-1-d31-acyl LPC were used to measure the activity of introduction into the *sn*-1 and *sn*-2 positions, respectively. Mean ± SEM. n = 3. *p<0.05, **p<0.01, ***p<0.001. Statistical analysis was done by one-way ANOVA with Tukey's test.

Figure 19

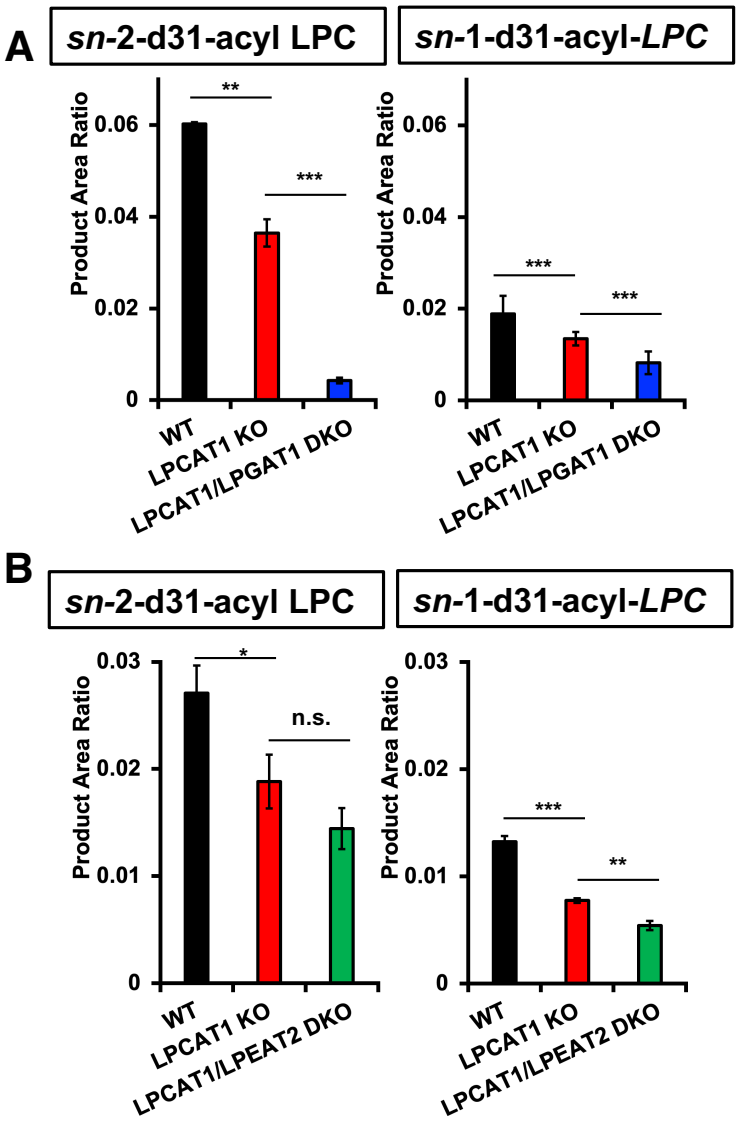

Fig. 19 DPPC synthesis activity is attenuated in LPCAT1/LPGAT1, LPCAT1/LPEAT2 DKO macrophages

(A) DPPC synthesis activity of LPCAT1/LPGAT1 DKO peritoneal macrophages. *sn*-2-d31-acyl LPC and *sn*-1-d31-acyl LPC were used to measure the activity of introduction into the *sn*-1 and *sn*-2 positions, respectively.

(B) DPPC synthesis activity of LPCAT1/LPEAT2 DKO macrophages. Mean ± SEM. n = 3. n.s., not significant. *p<0.05, **p<0.01, ***p <0.001. Statistical analysis was done by one-way ANOVA with Tukey's test.

Figure 20

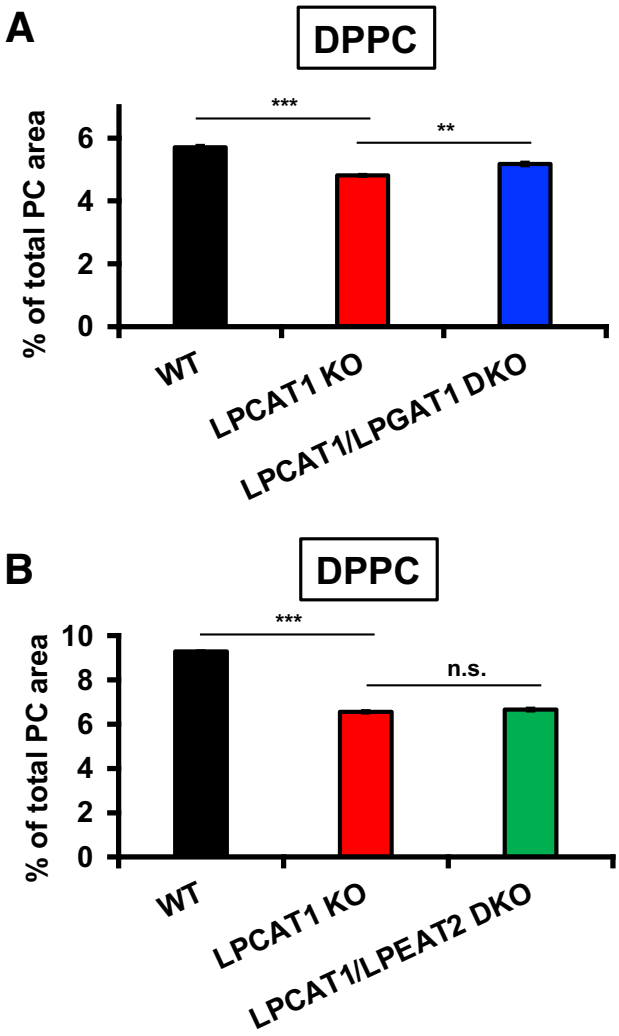

Fig. 20 DPPC is not reduced in LPCAT1/LPGAT1, LPCAT1/LPEAT2 DKO macrophages

(A) The amount of DPPC in LPCAT/LPGAT1 DKO peritoneal macrophages was analyzed by LC-MS/MS. Normalized peak area of the total amount and compositions of molecular species are shown. Mean ± SEM. n = 3.

(B) The amount of DPPC in LPCAT/LPEAT2 DKO peritoneal macrophages was analyzed by LC-MS/MS. Mean ± SEM. n = 3. n.s., not significant. **p<0.01, ***p <0.001. Statistical analysis was done by one-way ANOVA with Tukey's test.

Figure 21

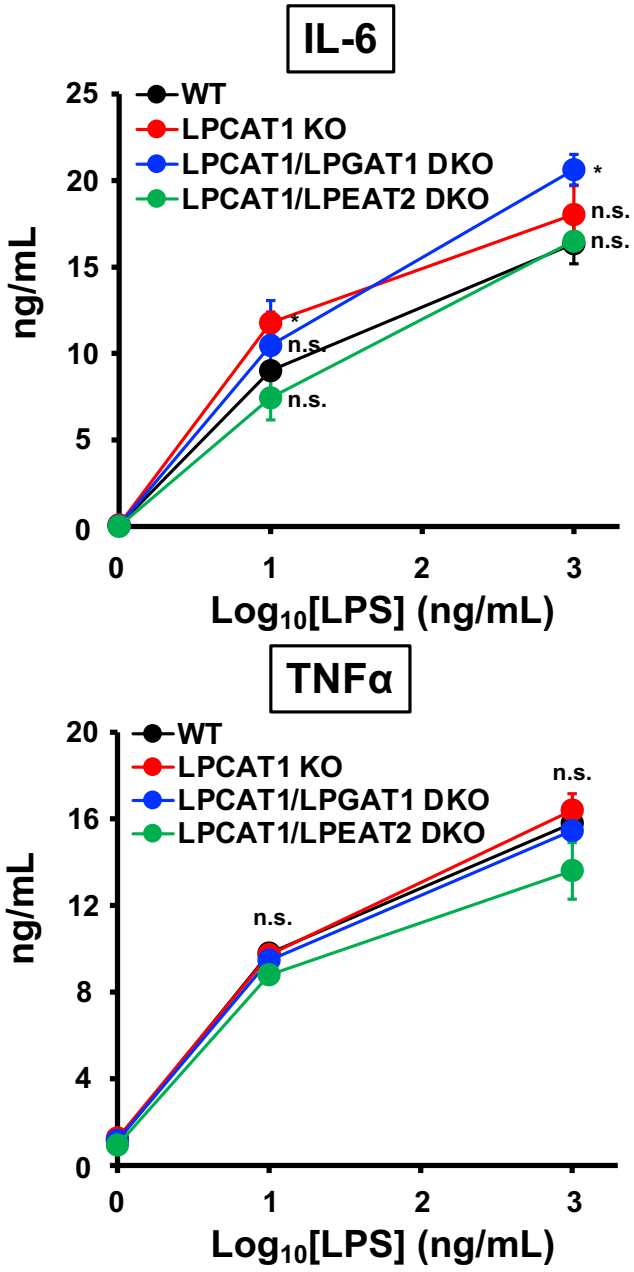

Fig. 21 LPS responsiveness is not altered in LPCAT1/LPGAT1, LPCAT1/LPEAT2 DKO macrophages

Cytokine secretion by LPCAT KO, LPCAT1/LPGAT1 DKO and LPCAT1/LPEAT2 DKO LPS-stimulated peritoneal macrophages. Mean ± SEM. n = 3.*$p<0.05$. Statistical analysis was done by one-way ANOVA with Tukey's test. Mean ± SEM. n = 3. n.s., not significant. *$p<0.05$. Statistical analysis was done by one-way ANOVA with Tukey's test.

Figure 22

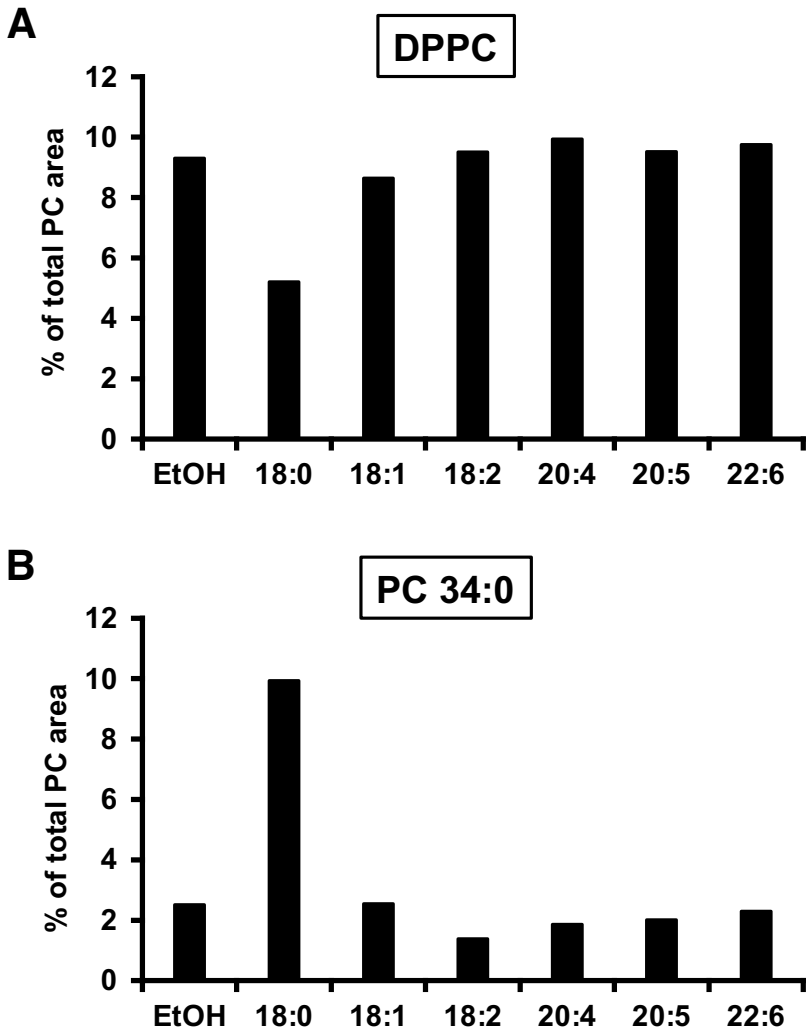

Fig. 22 Addition of 18:0 decreases DPPC but increases PC 34:0

(A) The amount of DPPC in peritoneal macrophages treated with each fatty acid was analyzed by LC-MS/MS. Normalized peak area of the total amount and compositions of molecular species are shown.
(B) The amount of PC 34:0 in peritoneal macrophages treated with each fatty acid was analyzed by LC-MS/MS. Normalized peak area of the total amount and compositions of molecular species are shown.

Figure 23

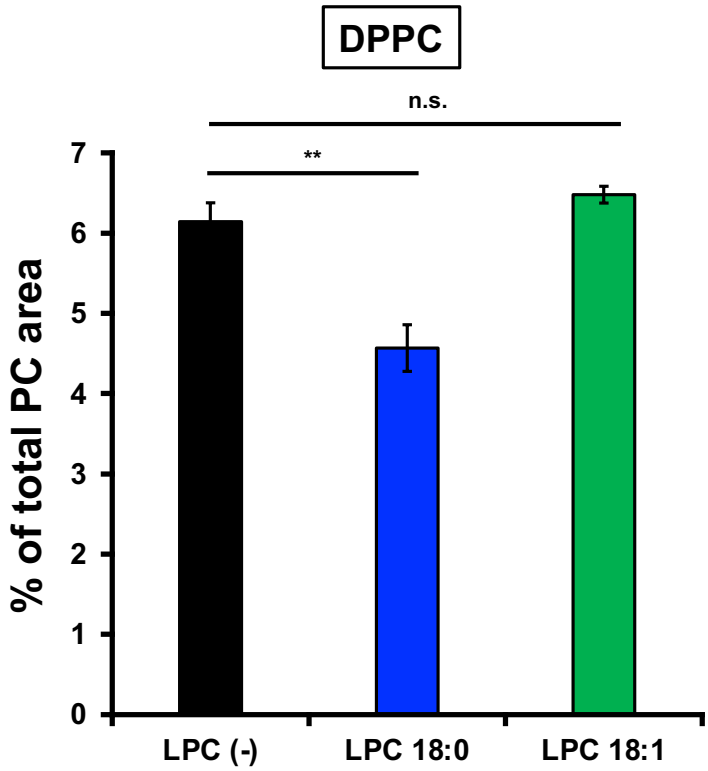

Fig. 23 DPPC is reduced by the addition of LPC 18:0

The amount of DPPC in peritoneal macrophages treated with each LPC was analyzed by LC-MS/MS. Normalized peak area of the total amount and compositions of molecular species are shown. Mean ± SEM. n = 3. n.s., not significant. **p<0.01. Statistical analysis was done by one-way ANOVA with Tukey's test.

Figure 24

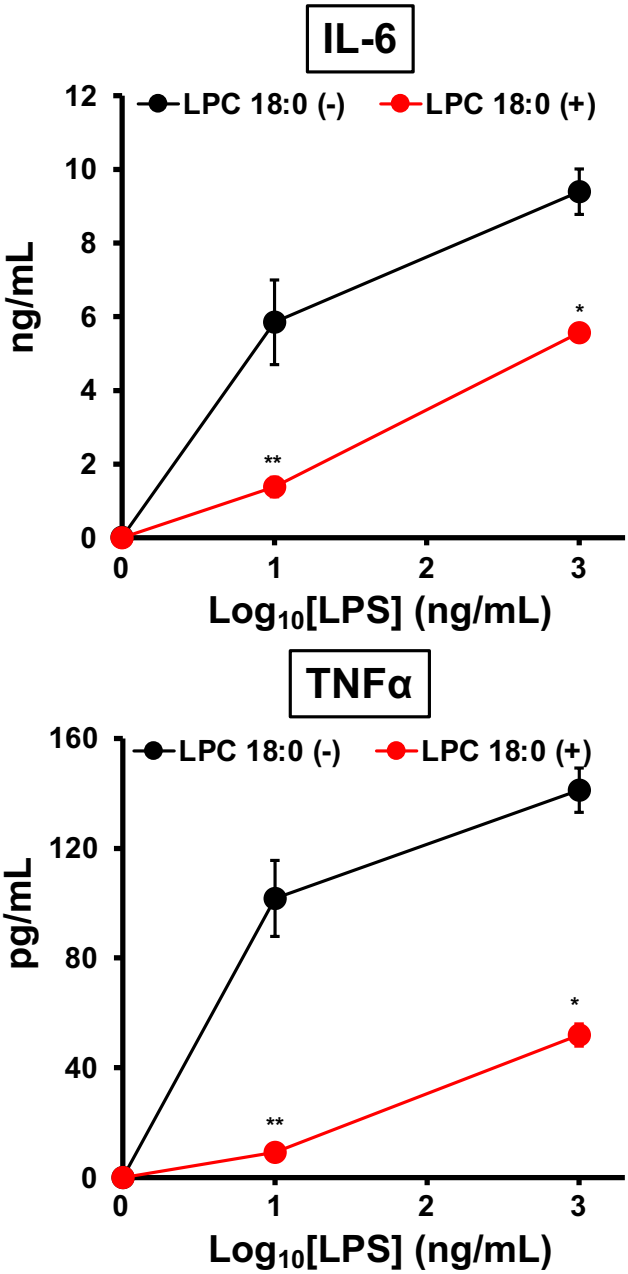

Fig. 24 Addition of LPC 18:0 attenuates LPS responsiveness

Cytokine secretion by peritoneal macrophages with LPC 18:0-treated and LPS-stimulated. Mean ± SEM. n = 3.*p<0.05. Statistical analysis was done by one-way ANOVA with Tukey's test. Mean ± SEM. n = 3. *p<0.05, **p <0.01. Statistical analysis was done by one-way ANOVA with Tukey's test.

Figure 25

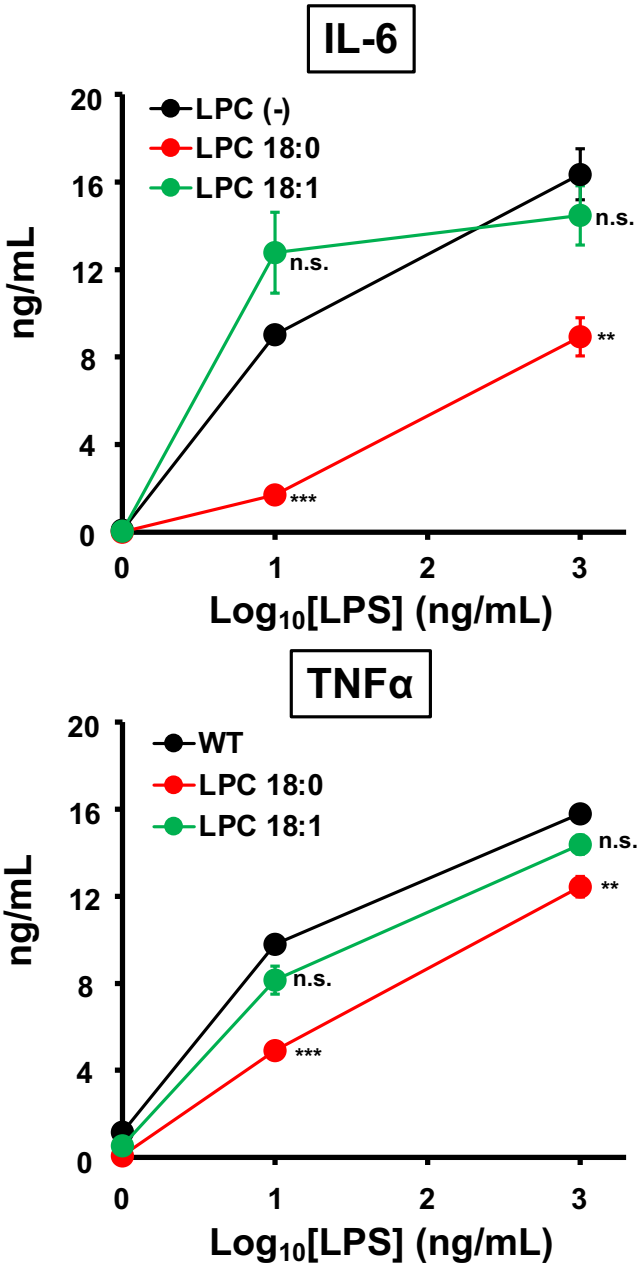

Fig. 25 LPS responsiveness is not attenuated by the addition of LPC 18:1

Cytokine secretion by peritoneal macrophages with LPC 18:1-treated and LPS-stimulated. Mean ± SEM. n = 3.*p<0.05. Statistical analysis was done by one-way ANOVA with Tukey's test. Mean ± SEM. n = 3. n.s., not significant. **p<0.01, ***p <0.001. Statistical analysis was done by one-way ANOVA with Tukey's test.

Figure 26

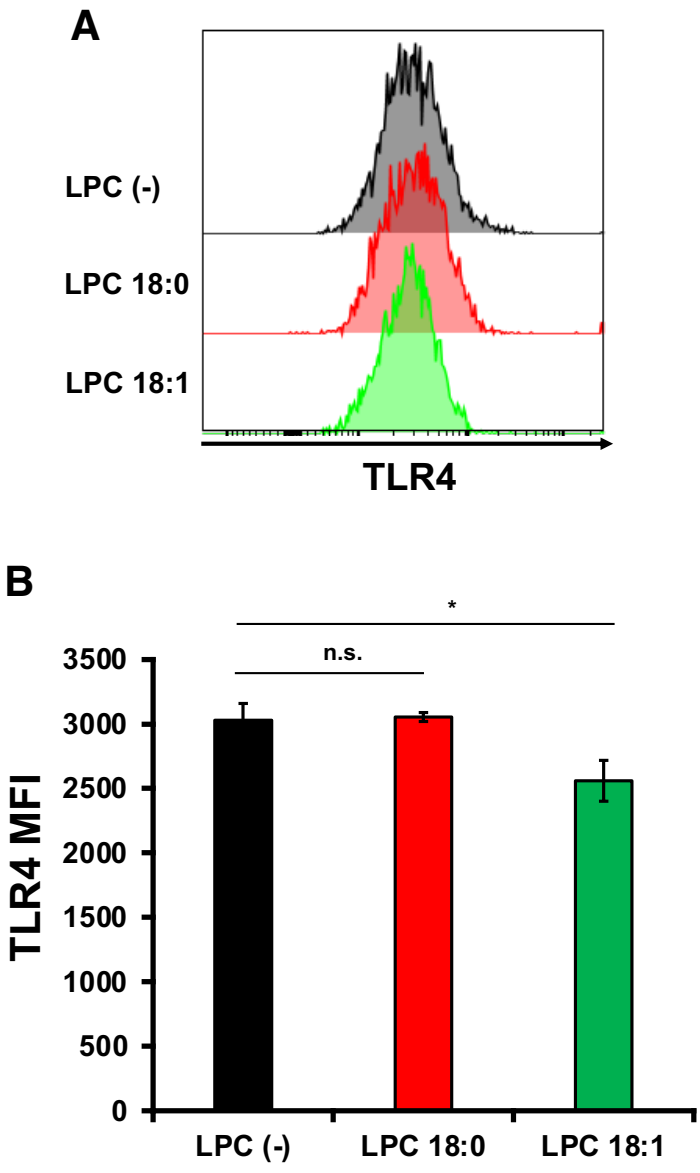

Fig. 26 Addition of LPC does not change the expression level of TLR4 on the cell surface

(A) Flow Cytometric analysis of TLR4 cell surface expression in LPC-treated peritoneal macrophages. TLR4 expression levels are shown as a histogram.

(B) Quantification result of Mean Fluorescence Intensity (MFI) of (A). Mean ± SEM. n = 3. n.s., not significant. *$p<0.05$. Statistical analysis was done by one-way ANOVA with Tukey's test.

Figure 27

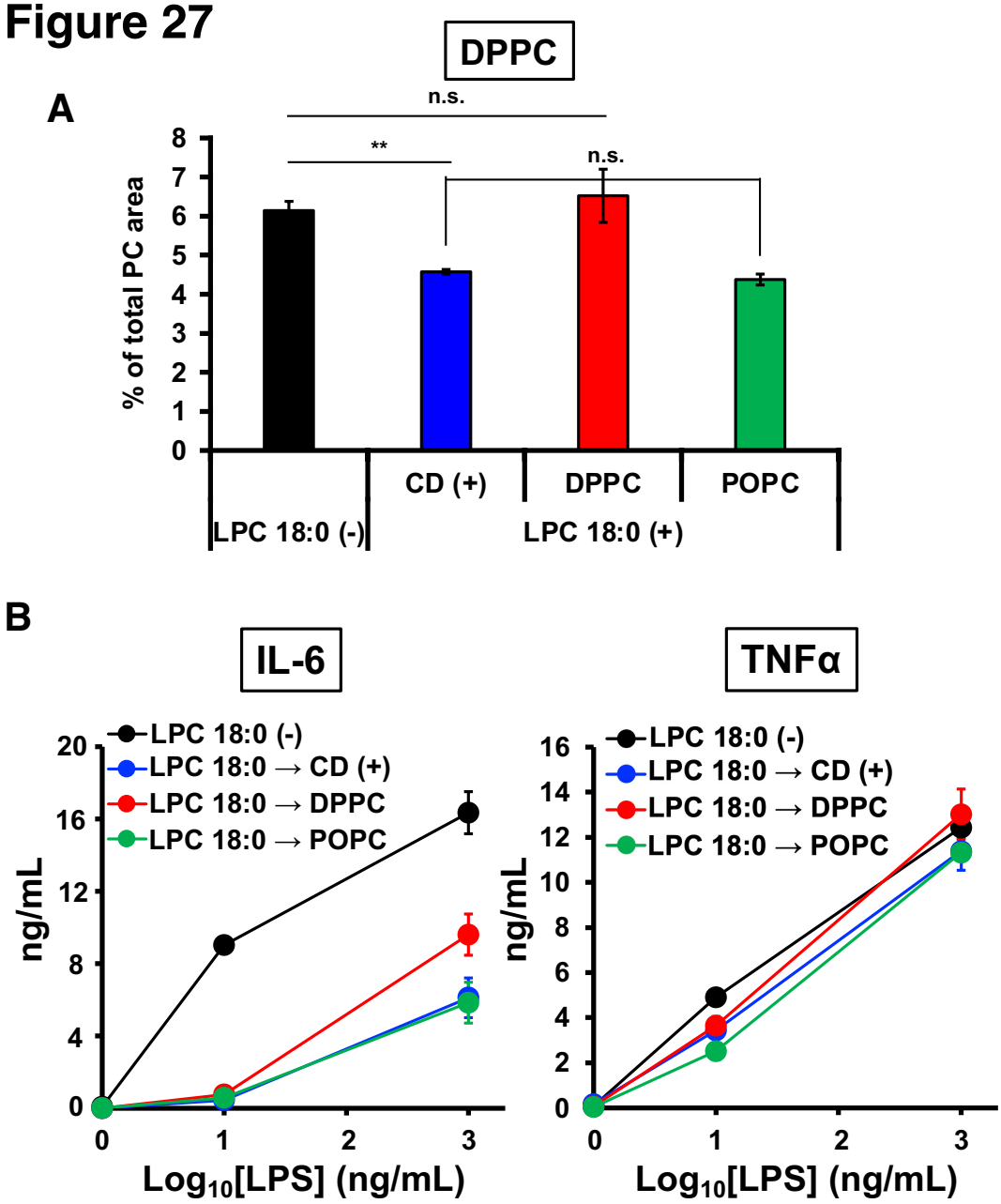

Fig. 27 Introduction of DPPC partially rescues the attenuation of LPS responsiveness by addition of LPC 18:0

(A) The amount of DPPC in peritoneal macrophages with treated LPC 18:0 followed by introduction of DPPC or POPC was analyzed by LC-MS/MS. Normalized peak area of the total amount and compositions of molecular species are shown. Mean ± SEM. n = 3. n.s., not significant. **p<0.01. Statistical analysis was done by one-way ANOVA with Tukey's test.

(B) Cytokine secretion by peritoneal macrophages introduced with DPPC or POPC and stimulated with LPS after LPC 18:0 treatment.

Figure 28

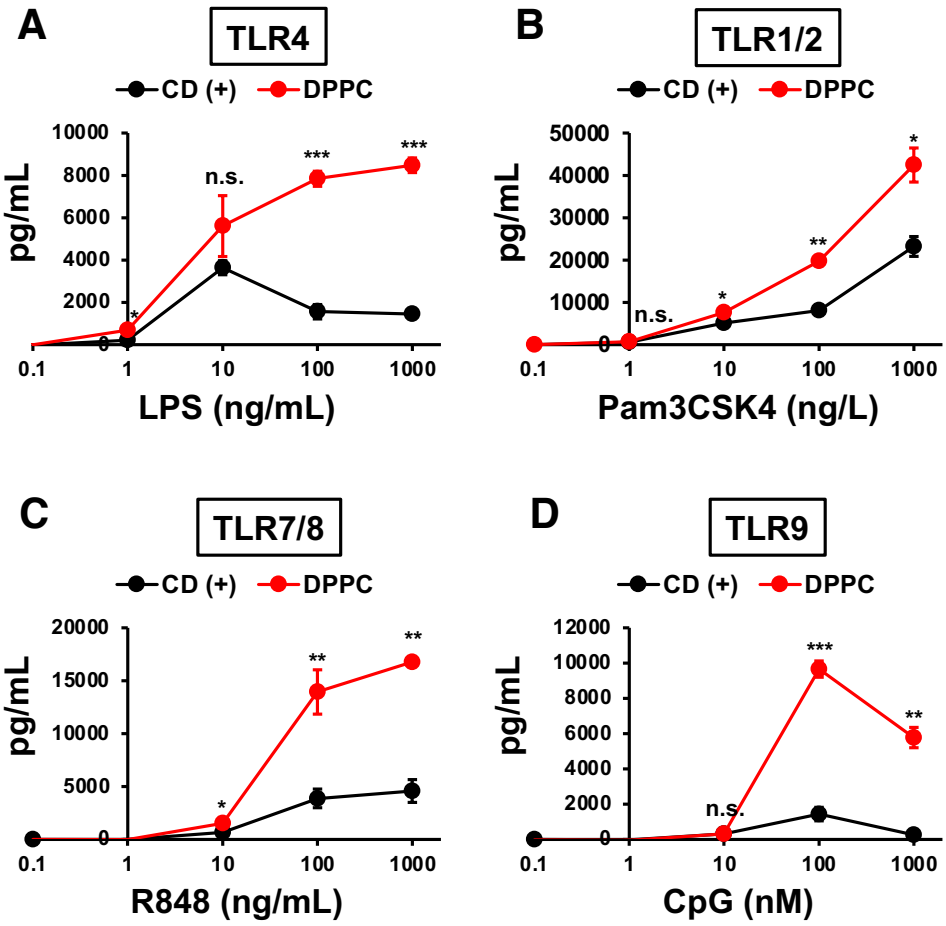

Fig. 28 DPPC enhances the responsiveness of TLRs

Cytokine secretion by DPPC-introduced and TLRs ligands-stimulated BMDMs. Mean ± SEM. n = 3. n.s., not significant. *p<0.05, **p<0.01, ***p <0.001. Statistical analysis was done by one-way ANOVA with Tukey's test.

Figure 29

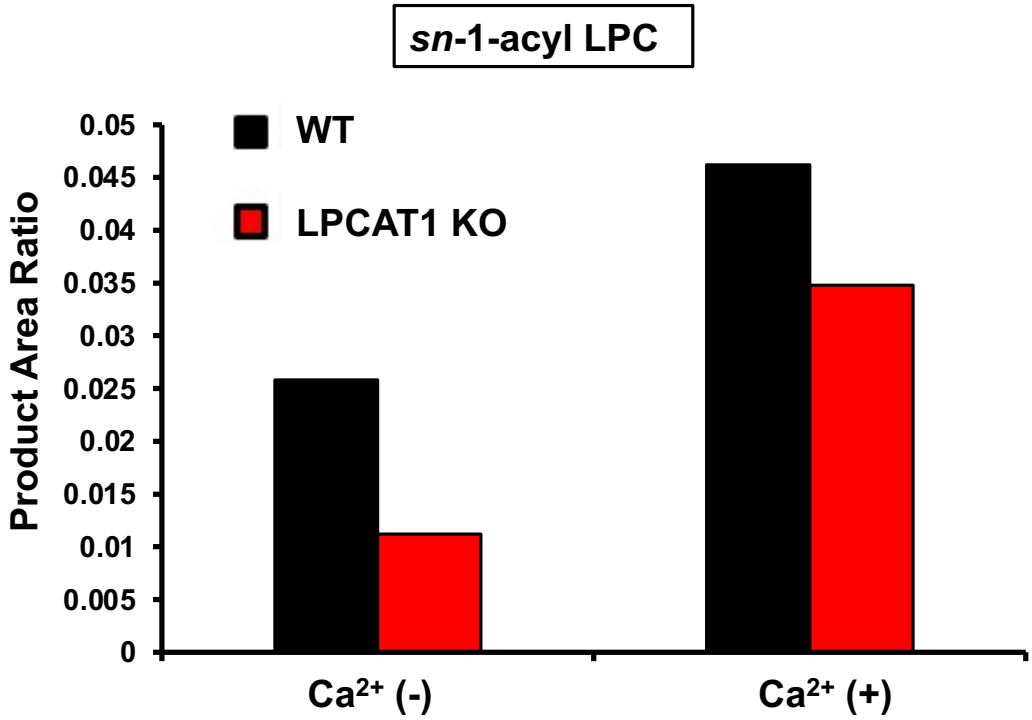

Fig. 29 DPPC synthetic activity in macrophages is Ca^{2+}-dependent

DPPC synthesis activity of LPCAT KO macrophages with or without Ca^{2+}. sn-1-acyl LPC was used to measure the activity of introduction into the sn-2 positions.

Table 1

【Ionization parameters】

Parameters	ZIC-HILIC	RPLC
Curtain Gas (psi)	10	10
Collision Gas (arb. Unit)	8	8
Ion Spray Voltage (V)	-4500	-4500
Temperature (℃)	600	700
Ion Source Gas 1 (psi)	50	30
Ion Source Gas 2 (psi)	70	70

【MS/MS parameters】

Phospholipid	HPLC condition	scan mode	DP (V)	EP (V)	CE (V)	CXP (V)
PS	ZIC-HILIC	NL 87 Da	-96	-10	-35.9	-15.4
PI		PIS m/z=241	-200	-10	-56	-9
PA, PG		PIS m/z=153	-140	-10	-44	-13
PC		NL 74 Da	-105	-10	-32	-19
PE		PIS m/z=196	-135	-10	-46.2	-15
DAG	RPLC	EMS	-11	-10	-31	-4

【MRM transitions】

Species	Q1	Q3	DP (V)	EP (V)	CE (V)	CXP (V)
DPPC	792.5	255	-100	-10	-62	-19
DPPE	690.5	255	-135	-10	-46	-15
DPPS	734.5	255	-96	-10	-36	-15
DPPI	809.5	255	-200	-10	-56	-9
DPPA	647.5	255	-130	-10	-42	-9
DPPG	721.5	255	-110	-10	-44	-13
d31-DPPC	823.5	286	-100	-10	-62	-19
d31-DPPE	721.5	286	-135	-10	-46	-15
d31-DPPS	765.5	286	-96	-10	-36	-15
d31-DPPI	840.5	286	-200	-10	-56	-9
d31-DPPA	678.5	286	-130	-10	-42	-9
d31-DPPG	752.5	286	-110	-10	-44	-13
d62-DPPC	854.5	286	-100	-10	-62	-19
d62-DPPE	752.5	286	-135	-10	-46	-15
d62-DPPS	796.5	286	-96	-10	-36	-15
d62-DPPI	871.5	286	-200	-10	-56	-9
d62-DPPA	709.5	286	-130	-10	-42	-9
d62-DPPG	783.5	286	-110	-10	-44	-13
d9-PC 30:0	715.5	193	171	10	37	14
d9-DPPC	743.5	193	171	10	37	14
d9-PC 34:1	769.5	193	171	10	37	14
d9-PC 34:0	771.5	193	171	10	37	14
d9-PC 38:4	825.5	193	171	10	37	14
$^{13}C_{16}$, d31-DPPC	781.5	184	171	10	37	14

Table 1 LC-MS/MS parameters and MRM transitions used in this study

NL, neutral loss scan; PIS, precursor ion scan; EMS, enhanced MS scan; DP, declustering potential; EP, entrance potential; CE, collision energy; CXP, collision cell exit potential

Table 2

Name	Target sequences
GFP	GAAGCTGACCCTGAAGTTCATC
Cpt1 #1	GGACTATACGATACCTATTCT
Cpt1 #5	GTCATTTCTTCATTTGATATG
Cept1 #4	GCTTCATTGATGAATATATAG
Cept1 #5	GGAACATTGCGATTTGGAATA
Lpgat1 #4	GAATTGTTTCTCTTATTCATG
Lpgat1 #5	GAACCAATAGACATTCAGACC
Lpeat2 #1	CACTGAATGTGAGTTTGTAGG
Lpeat2 #3	GTAAAAGACTATTTTATATAT

Table 2 Target sequence of shRNA

Table 3

【qRT-PCR primers】

Name	Forward primer	Reverse primer
18S	5'-GTAACCCGTTGAACCCCATT-3'	5'-CCATCCAATCGGTAGTAGCG-3'
Cpt1	5'-TTCATGTCAACAAGCACCGGAACAG-3'	5'-ACAGCAGCAGCAAGAGATGGCAAA-3'
Cept1	5'-AGGCTTGTGCTTGTTGGGTTCGG-3'	5'-CGATGCCCACTCATGGAGCTTGGTT-3'
Lpgat1	5'-TGGAGATGTGCCCTTGGAGACCGA-3'	5'-TGCACACAGCTTCCTTCTGGCCCT-3'
Lpeat2	5'-ATGAGTTACACCTCTCCGGCCTCCA-3'	5'-ACGCGAAGGGCCAGAGGAGAAAGA-3'

【cloning primers】

Name	Accession No.	Forward primer	Reverse primer
Lpcat1	NM_145376	5'-AAGGATGACGATGATAAGAGGCTGCGGGGCCGCGGGCC-3'	5'-CATTGGCCATCGATCTCGAGCTAGTCCGCTTTCTTACAAG-3'
Lpaat1	NM_001163379	5'-AAGGATGACGATGATAAGGAGCTGTGGCCCGGGGCCTG-3'	5'-CATTGGCCATCGATCTCGAGTCAGAGCCGGGCTTCGCCCG-3'
Lpaat2	NM_026212	5'-AAGGATGACGATGATAAGGACCCGTGGCCATGGCTGAC-3'	5'-CATTGGCCATCGATCTCGAGCTACTGGGCTGGCAAGACCC-3'
Lpaat3	NM_053014	5'-AAGGATGACGATGATAAGGGCCTGCTTGCCTACCTGAA-3'	5'-CATTGGCCATCGATCTCGAGTTATTCCTTTTTCTTAAGCT-3'
Agpat4	NM_026644	5'-AAGGATGACGATGATAAGGACCTCATCGGGCTGCTGAA-3'	5'-CATTGGCCATCGATCTCGAGTCAGTCCGTTTGTTTCCGTT-3'
Lpcat2	NM_173014	5'-AAGGATGACGATGATAAGAACCGATGCGCCGAGGCGGC-3'	5'-CATTGGCCATCGATCTCGAGTCAGTCCACCTTTTTGTCTG-3'
Lpcat2b	NM_027599	5'-AAGGATGACGATGATAAGGCTCATCAGAACCAGCACCA-3'	5'-CATTGGCCATCGATCTCGAGTTATACTTCTCTTGGTAATG-3'
Lpeat2	NM_207206	5'-AAGGATGACGATGATAAGAGCCAGGGAAGTCCTGGGGC-3'	5'-CATTGGCCATCGATCTCGAGTCAGTCTCCCTTCTGCTTGG-3'
Lclat1	NM_001081071	5'-AAGGATGACGATGATAAGGTGTCATGGAAGGGGATTTA-3'	5'-CATTGGCCATCGATCTCGAGTTACTCATTTTTCTTTGAAT-3'
Lpgat1	NM_001134829	5'-AAGGATGACGATGATAAGACCGCGACCCCCGGGCCAGG-3'	5'-CATTGGCCATCGATCTCGAGCTAAAATAGACAATGGTAAA-3'
Lpcat3	NM_145130	5'-AAGGATGACGATGATAAGGCGTCTACAGCGGACGGGGA-3'	5'-CATTGGCCATCGATCTCGAGTCATTCCCTCTTTTTTAACT-3'
Lpcat4	NM_026037	5'-AAGGATGACGATGATAAGGCCACCACCAGCACCACGGG-3'	5'-CATTGGCCATCGATCTCGAGTCACTGTGTTAGTGACGAGT-3'
Lpeat1	NM_153546	5'-AAGGATGACGATGATAAGGCAGCACGGCCGCCCGCCAG-3'	5'-CATTGGCCATCGATCTCGAGTCAGTCTGCCTTCTTCTTTA-3'
Lpiat1	NM_029934	5'-AAGGATGACGATGATAAGACACCCGAAGAATGGACATA-3'	5'-CATTGGCCATCGATCTCGAGTCACTCTTCCCGGAGCTTTT-3'

Table 3　Primers used in this study

Materials and Methods

Materials

All chemicals were purchased from Wako Pure Chemicals (Osaka, Japan) unless otherwise stated.

Animals

Mice were housed in an air-conditioned room (23 ± 1 ℃) under 12 hr dark/12 hr light cycles. Studies using mice were approved and performed in accordance with the guidelines of the animal experimentation committee of the University of Tokyo.

Antibody

Antibody to GAPDH (6C5) was purchased from Calbiochem, Merck Millipore (Darmstadt, Germany). Antibody to LPCAT1 (NBP1-88923) was purchased from Novus. Antibody to Calnexin was purchased from Enzo Lifesciences. Antibody to FLAG (1E6) was purchased from Wako.

MS analysis of phospholipids

Frozen tissues samples were pulverized, and lipids were extracted using the method of Bligh and Dyer[51]. Phospholipids were extracted from cells in the same way. The amount of phospholipids was quantitated by phosphorus assay[52]. The phosphorus concentration of the sample was adjusted to 300 μM, and each internal standard was added at 1 μM. The high-performance liquid chromatography-electrospray ionization-tandem mass spectrometry (LC-ESI-MS/MS) analysis was performed on a Shimadzu Nexera ultra high-performance liquid chromatography system (Shimadzu, Kyoto, Japan) coupled with

a QTRAP 4500 hybrid triple quadrupole linear ion trap mass spectrometer (AB SCIEX, Framingham, MA). Lipids were injected by an autosampler; typically, 10 µl (3 nmol phosphorus equivalent) of the sample was applied. For the lipid analysis chromatographic separation was performed on a SeQuant ZIC-HILIC column (250 × 2.1 mm, 3.5 µm; Merck, Berlin, Germany) maintained at 50 ℃ using mobile phase A [acetonitrile/water (95:5, v/v)] and mobile phase B [acetonitrile/water (50:50, v/v) containing 20mM ammonium acetate] in a gradient program (0-22 min: 0-40% B; 22-25 min: 40% B; 25-30 min: 0% B) with a flow rate of 0.3 ml/min. For the analysis of DAG, reverse-phase chromatographic separation was performed as previously described[52]. PC and PE were measured in the positive ion mode, while other phospholipids were in the negative ion mode. Phospholipids were identified by the ionization pattern, which was characteristic for each headgroup. The instrument parameters were listed in Table 1. Internal standards were as follows: 12:0-13:0 phosphatidylcholine (PC), 12:0-13:0 phosphatidylethanolamine (PE), 12:0-13:0 phosphatidylserine (PS), 12:0-13:0 phosphatidylinositol (PI), 12:0-13:0 phosphatidylglycerol (PG) (Avanti Polar Lipids, Birmingham, AL). Specific detection was performed by MRM as described in Table1.

Isolation of adipose tissue macrophage from white adipose tissue

Single-cell suspensions of white adipose tissue were prepared as previously described[53] with slight modifications. The mice were euthanized by appropriate procedures. The thoracic cavity was opened to expose the heart. A cardiac perfusion was performed to remove blood from tissues with PBS. The perigonadal adipose tissue was collected in FACS buffer (2% FBS, 2 mM EDTA in PBS), and mince with scissors. Collagenase was added to the adipose tissue at a final concentration of 1 mg/mL, and incubated them with

shaking for 30 minutes at 37℃. EDTA was added to adipose tissue at a final concentration of 10 mM, and incubated them with shaking for another 30 minutes. The adipose tissue were centrifuged at 500 g at 4℃ for 10 minutes, resuspended with FACS buffer, and filtrated through a 100 μm filter (BD Biosciences). Filtered samples were centrifuged at 500 g at 4℃ for 10 minutes, and the pellets were resuspended with red blood cell lysis buffer (Sigma) and incubated for 5 minutes. After adding FACS buffer, samples were centrifuged at 500 g at 4℃ for 10 minutes, and the pellets were resuspended in FACS buffer. The cell suspension were incubated with anti-CD16/32 (2.4G2, TONBO Biosciences) for 10 minutes to inhibit non-specific binding, followed by incubation with the antibody mixture for 30 minutes. The following antibodies were used for cell sorting: from TONBO Biosciences: PE-Cy7-CD45 (30-F11); from BioLegend: FITC-CD11b (M1/70), and APC-F4/80 (BM8); from BD Biosciences: BV421-siglec-F (E50-2440). Flow cytometry measurements and cell sorting were performed on a FACS Aria II cell sorter. The following gating strategy was used: doublets were excluded based on forward scatter-A against forward scatter-W, followed by side scatter-A against side scatter-W. Next, adipose tissue leukocytes (CD45+) were selected. To exclude eosinophils contained in F4/80, CD11b positive cells, siglec-F negative cells were isolated as adipose tissue macrophages.

Isolation of thioglycolate induced peritoneal macrophage

Mouse peritoneal macrophages were isolated as described elsewhere[54]. In brief, 4 days after intraperitoneal injection of 2 ml 4% thioglycollate, peritoneal macrophages were harvested from the peritoneal cavity with ice-cold PBS. Cells (2.0×10^6 cells/well on a 6-well plate and 1.0×10^6 cells/well on a 12-well plate) were cultured in RPMI1640

medium (Thermo) supplemented with 10% FBS (Gibco) and Penicillin-Streptomycin-Glutamine (PSG) (Gibco) at 37°C in a humidified atmosphere of 5% CO2.

Phospholipid introduction to cells

Phospholipids in chloroform were dried with nitrogen gas. RPMI-1640 (FBS (-), PSG(-)) was added to the dried phospholipids and sonicated for 30 minutes at room temperature. Then the solution was centrifuged at 3000 g at room temperature for 5 minutes. Add methyl alpha-cyclodextrin (40mM stock in PBS) and RPMI (10% FBS, PSG) in the ratio 5:2:3. The final lipid concentration is 30 μM to the supernatant.

Cell culture

BMDMs and peritoneal macrophages were cultured with RPMI1640 (10% FBS, PSG). HEK293T cells were cultured with Dulbecco's Modified Eagle's Medium (DMEM) (Sigma-Aldrich) supplemented with 10% FBS and PSG.

Differentiation of BMC to BMDM

BMCs of tibias and femur from C57BL6/J wild-type mice (male, 6 to 8 weeks old) (CLEA Japan, Inc.) were flushed out with RPMI1640 (PSG). The cells were collected by centrifugation at 300 g for 5 min, resuspended with RPMI1640 (10% FBS, PSG), and filtrated with a 40 μm cell strainer (BD Biosciences). The cells were seeded at 13.1 x 10^6 cells on a 10 cm dish for 2 hours at 37˚C, 5% CO_2. After 2 hours, floating cells were collected by centrifugation at 300 g for 5 min. Cells were counted and seeded at 1.31 x 10^6 cells/cm2 with 15% L929 conditioned medium at 10 cm RepCell (CellSeed) (day 0). The medium was changed on day 3. On day 6, cells were collected with ice-cold PBS and

seeded at 3.0×10^6 cells/well on a 6-well plate.

LPS treatment

LPS-EB (InvivoGen) was diluted in a culture medium and added to cells. After 24 hours, the culture supernatant was collected and centrifuged at 400 g at 4°C for 5minutes to remove cells, and at 3000 g for at 4°C 5min to remove debris. The amount of pro-inflammatory cytokines in the culture supernatant was quantified by ELISA.

ELISA

For measurements of IL-6 and TNFα in culture supernatants, we used the BD OptEIA™ ELISA Set according to the manufacturer's protocol (BD Biosciences).

Measurement of the ability to synthesize palmitate-containing PC using d31-labeled palmitate

Palmitic acid-d31 (d31-16:0) (Cayman) was diluted in 0.5% BSA RPMI1640 to 10 μM and added to cells. Lipids were extracted at each time point, and d31-16:0-containing phospholipids were measured by LC-MS/MS. Calibration curves were drawn using DPPC, DPPE, DPPS, DPPA, DPPI, and DPPG standards (Avanti) to calculate the amount synthesized d31-16:0 labeled phospholipids. Specific detection was performed by MRM as described in Table2.

Preparation of lentivirus for gene suppression in macrophage

HEK293T cells were transfected with pLKO.1 puro (Addgene) vector containing shRNA, psPAX2, and pMD2.G using LipofectamineLTX (Invitrogen), according to the

manufacturer's protocol. The medium was changed 4-6 hours after transfection, and the cells were cultured for another two days. The insert sequences were listed in Table3.

Lentivirus induction into peritoneal macrophages

Peritoneal macrophages were seeded in a 6-well plate or 12-well plate. On the next day, the medium was changed to a lentivirus solution supplemented with polybrene (8 μg/mL) (Sigma-Aldrich), and the culture plates were centrifuged at 1,200 g for 90 minutes at room temperature. The medium was replaced with RPMI 1640 (10% FBS, PSG) after centrifugation. The cells were further cultured for 48 hours and then selected with RPMI (10% FBS, PSG) containing 3 μg/ml puromycin for 3 days.

Measurement of de novo synthesis of PC using d9-labeled choline

Choline-d9 chloride (Toronto) was diluted in choline-deficient RPMI1640 () to 1 μg/mL and added to cells. After 1 hour, Lipids were extracted, and d9-choline-containing PCs were measured by LC-MS/MS. Specific detection was performed by MRM as described in Table2.

Preparation of membrane fractions

For membrane preparation, cells were washed with buffer A1 (20 mM Tris-HCl (pH 7.4) and 300 mM sucrose) and scraped in buffer A2 (buffer A1 plus 1 x complete protease inhibitor cocktail (Nacalai)) prior to sonication. Cells were disrupted on ice using a probe sonicator for 20 x 5 seconds. Sonicated samples were then centrifuged at 800 g for 10 minutes. Then, the supernatants were ultracentrifuged at 100,000 g for 1 hour. Pellets

were resuspended in buffer A4 (20 mM Tris-HCl (pH 7.4), 300 mM sucrose, and 1 mM EDTA), and protein concentrations were determined by the BCA assay (Pierce).

DPPC synthesis activity assay

DPPC synthesis activity that introduce palmitic acid into palmitoyl LPC was determined by measuring the product of the this reaction with a slight modification[29]. In this reaction, membrane fractions, LPC (*sn*-1-d31-palmitoyl dominant LPC (*sn*-1-d31-acyl LPC) or *sn*-2-d31-palmitoyl dominant LPC (*sn*-2-acyl LPC) and $^{13}C_{16}$-palmitoyl-CoA were mixed and incubated at 37 °C for 10 min. The final reaction mixture contained 110 mM Tris-HCl (pH 7.4), 150 mM sucrose, 0.5 mM EDTA, 10 μM LPC, 2 μM Acyl-CoA, 0.015% Tween-20 and 0.1 μg of membrane protein. The reaction was stopped by adding chloroform/methanol (1:2). 12:0-13:0 PC was added as an internal standard and lipids were extracted by the Bligh & Dyer method. The organic (lower) layer was evaporated, dissolved in isopropanol/methanol (1:1), and the amounts of DPPC containing both $^{13}C_{16}$ and d31-labeled palmitic acid was quantified by LC–MS/MS. Measurements were performed in the negative ion mode. Specific detection was performed by MRM as described in Table2.

Cloning of LPLAT

cDNA for mouse LPLAT was amplified by using KOD One PCR Master Mix (TOYOBO) and DNA template from mouse brain, liver, peritoneal macrophage cDNA as a template. The primers used for cloning these enzymes are shown in Table4. The amplified cDNA fragments were inserted into the pCAGGS vector (a gift from J. Miyazaki, Osaka

University) with an N-terminal FLAG-tag. The nucleotide sequences of all the plasmids prepared were checked by DNA sequencing.

Establishment of LPCAT1 KO HEK293T cell

To generate LPCAT1 KO HEK293T cells using CRISPR)/Cas9 technology[55], a DNA fragment encoding guide RNA of LPCAT1 (sense, 5′-CACCGGTTCGCCGGCGGCTTCCAC-3′; antisense, 5′-AAACGTGGAAGCCGCCGGCGAACC-3′) was cloned into pX458 vector (Addgene). Cells were transfected with the vector using Lipofectamine 2000 transfection reagent (Invitrogen) according to the manufacturer's instructions. Forty-eight hours after transfection, the GFP positive cells were sorted by the cell sorter SH800 (SONY) and cultured, and then, the cells were plated as single colonies in 96-well plates. The clones that no longer expressed LPCAT1 protein were selected by WB. The clones with the most attenuated DPPC synthetic activity were selected by LPCAT assay and used for the subsequent experiments.

Transfection of plasmids

HEK293A cells were transfected with cDNAs encoding several LPLATs using Opti-MEM and Lipofectamine 2000 (Thermo FisherScientific)

LPC and fatty acid treatment

LPC in methanol was dried with nitrogen gas. RPMI-1640 (10%FBS, PSG) was added to the dried LPC and sonicated for 1 minute at room temperature. The LPC solution was added to the cells. After 24 hours, the cells were treated LPS, extracted lipids, and

measured cell surface TLR4 expression. Stearic acid (18:0), oleic acid (18:1), linoleic acid (18:2), arachidonic acid (20:4), eicosapentaenoic acid (EPA, 20:5) and docosahexaenoic acid (DHA, 22:6) in ethanol (EtOH) were diluted in 0.5% BSA RPMI1640 to 100 μM and added to cells. After 4 hours, the cells were treated LPS and extracted lipids.

Western blotting

Cells were collected with lysis buffer (20 mM Tris-HCl pH 7.4, 100 mM NaCl, 5 mM EDTA, 1% TritonX100, 0.1% SDS) with protease inhibitor cocktail (Nacalai) and phosphatase inhibitors (5 mM NaF and 2 mM sodium orthovanadate). After incubation at 4 ˚C for 20 minutes, the lysate was centrifuged at 12,000 rpm at 4 ˚C to remove the insoluble fraction. The supernatant was used as the protein extracts. The protein concentrations were determined by the BCA assay.

Proteins were separated by SDS-PAGE and transferred to PVDF membranes. The membranes were blocked with 5% BSA in TTBS buffer (10 mM Tris-HCl pH 7.4, 150 mM NaCl, 0.1 % Tween 20) and incubated with primary antibodies overnight at 4 ˚C. On the next day, the membranes were incubated with horseradish peroxidase-conjugated anti-mouse or anti-rabbit IgG antibody (GE Healthcare). The proteins were detected by enhanced chemiluminescence (ECL Western blotting detection system, GE Healthcare) using LAS4000 (GE Healthcare Life Sciences).

Cell surface TLR4 expression analysis by flow cytometry

Samples were constantly handled on ice or at 4℃, avoiding direct light exposure. First, samples were incubated with Live/Dead Fixable Violet Dead Cell Stain (ThermoFisher)

or Fixable Viability Dye eF506 (eBioscience) in PBS for 10 min to exclude nonviable cells. Next, samples were incubated for 10 min with rat anti CD16/CD32 in FACS buffer to block FcγRIII/II and reduce unspecific antibody binding. Then, cell suspensions were incubated for 30 min with an antibody cocktail in FACS buffer. For cell surface antigens, the following anti-mouse antibodies were used: from BioLegend: FITC-CD11b (M1/70), APC-F4/80 (BM8), and PE-TLR4 (SA15-21).

qRT-PCR

Total RNA was extracted from cells with ISOGEN II (Nippon Gene) and reverse transcribed with High-Capacity cDNA Reverse Transcription Kit (Applied Biosystems, Thermo Fisher Scientific) according to the manufacturer's protocol. RT-PCR analysis was performed with LightCycler 480 II (Roche) or LigftCycler 96 (Roche), using SYBR Premix Ex Taq II (Takara Bio) or KAPA SYBR FAST One-Step qRT-PCR Kit (NIPPON Genetics Co., Ltd). The primers used in RT-PCR are listed in Table5.

References

1 Harayama, T. & Riezman, H. Understanding the diversity of membrane lipid composition. *Nat Rev Mol Cell Biol* **19**, 281-296, doi:10.1038/nrm.2017.138 (2018).

2 Contreras, F. X., Ernst, A. M., Wieland, F. & Brugger, B. Specificity of Intramembrane Protein-Lipid Interactions. *Cold Spring Harbor Perspectives in Biology* **3**, doi:10.1101/cshperspect.a004705 (2011).

3 Contreras, F. X. *et al.* Molecular recognition of a single sphingolipid species by a protein's transmembrane domain. *Nature* **481**, 525-529, doi:10.1038/nature10742 (2012).

4 De Craene, J. O., Bertazzi, D. L., Bar, S. & Friant, S. Phosphoinositides, Major Actors in Membrane Trafficking and Lipid Signaling Pathways. *International Journal of Molecular Sciences* **18**, doi:10.3390/ijms18030634 (2017).

5 Laganowsky, A. *et al.* Membrane proteins bind lipids selectively to modulate their structure and function. *Nature* **510**, 172-+, doi:10.1038/nature13419 (2014).

6 Lingwood, D. *et al.* Cholesterol modulates glycolipid conformation and receptor activity. *Nature Chemical Biology* **7**, 260-262, doi:10.1038/nchembio.551 (2011).

7 Spector, A. A. & Yorek, M. A. Membrane lipid composition and cellular function. *J Lipid Res* **26**, 1015-1035 (1985).

8 Yang, Y., Lee, M. & Fairn, G. D. Phospholipid subcellular localization and dynamics. *J Biol Chem* **293**, 6230-6240, doi:10.1074/jbc.R117.000582 (2018).

9 Shindou, H. *et al.* Docosahexaenoic acid preserves visual function by

maintaining correct disc morphology in retinal photoreceptor cells. *J Biol Chem* **292**, 12054-12064, doi:10.1074/jbc.M117.790568 (2017).

10 Pichot, R., Watson, R. L. & Norton, I. T. Phospholipids at the Interface: Current Trends and Challenges. *International Journal of Molecular Sciences* **14**, 11767-11794, doi:10.3390/ijms140611767 (2013).

11 KENNEDY, E. P. The synthesis of cytidine diphosphate choline, cytidine diphosphate ethanolamine, and related compounds. *J Biol Chem* **222**, 185-191 (1956).

12 Kennedy, E. P. THE BIOLOGICAL SYNTHESIS OF PHOSPHOLIPIDS. *Canadian Journal of Biochemistry and Physiology* **34**, 334-348, doi:10.1139/o56-036 (1956).

13 Hishikawa, D., Hashidate, T., Shimizu, T. & Shindou, H. Diversity and function of membrane glycerophospholipids generated by the remodeling pathway in mammalian cells. *Journal of Lipid Research* **55**, 799-807, doi:10.1194/jlr.R046094 (2014).

14 Yamashita, A. *et al.* Acyltransferases and transacylases that determine the fatty acid composition of glycerolipids and the metabolism of bioactive lipid mediators in mammalian cells and model organisms. *Progress in Lipid Research* **53**, 18-81, doi:10.1016/j.plipres.2013.10.001 (2014).

15 LANDS, W. E. Metabolism of glycerolipides; a comparison of lecithin and triglyceride synthesis. *J Biol Chem* **231**, 883-888 (1958).

16 Yamashita, A., Sugiura, T. & Waku, K. Acyltransferases and transacylases involved in fatty acid remodeling of phospholipids and metabolism of bioactive lipids in mammalian cells. *Journal of Biochemistry* **122**, 1-16 (1997).

17 Henneberry, A. L., Wright, M. M. & McMaster, C. R. The major sites of cellular phospholipid synthesis and molecular determinants of fatty acid and lipid head group specificity. *Molecular Biology of the Cell* **13**, 3148-3161, doi:10.1091/mbc.01-11-0540 (2002).

18 Henneberry, A. L., Wistow, G. & McMaster, C. R. Cloning, genomic organization, and characterization of a human cholinephosphotransferase. *J Biol Chem* **275**, 29808-29815, doi:10.1074/jbc.M005786200 (2000).

19 Henneberry, A. L. & McMaster, C. R. Cloning and expression of a human choline/ethanolaminephosphotransferase: synthesis of phosphatidylcholine and phosphatidylethanolamine. *Biochemical Journal* **339**, 291-298, doi:10.1042/0264-6021:3390291 (1999).

20 Horibata, Y. & Sugimoto, H. Differential contributions of choline phosphotransferases CPT1 and CEPT1 to the biosynthesis of choline phospholipids. *Journal of Lipid Research* **62**, doi:10.1016/j.jlr.2021.100100 (2021).

21 Shindou, H., Hishikawa, D., Harayama, T., Yuki, K. & Shimizu, T. Recent progress on acyl CoA: lysophospholipid acyltransferase research. *Journal of Lipid Research* **50**, S46-S51, doi:10.1194/jlr.R800035-JLR200 (2009).

22 Hishikawa, D. *et al.* Discovery essential of a lysophospholipid acyltransferase family for membrane asymmetry and diversity. *Proceedings of the National Academy of Sciences of the United States of America* **105**, 2830-2835, doi:10.1073/pnas.0712245105 (2008).

23 Harayama, T., Shindou, H., Ogasawara, R., Suwabe, A. & Shimizu, T. Identification of a novel noninflammatory biosynthetic pathway of platelet-

activating factor. *Journal of Biological Chemistry* **283**, 11097-11106, doi:10.1074/jbc.M708909200 (2008).

24 Holm, B. A., Wang, Z. D., Egan, E. A. & Notter, R. H. Content of dipalmitoyl phosphatidylcholine in lung surfactant: Ramifications for surface activity. *Pediatric Research* **39**, 805-811, doi:10.1203/00006450-199605000-00010 (1996).

25 Veldhuizen, R., Nag, K., Orgeig, S. & Possmayer, F. The role of lipids in pulmonary surfactant. *Biochimica Et Biophysica Acta-Molecular Basis of Disease* **1408**, 90-108, doi:10.1016/s0925-4439(98)00061-1 (1998).

26 Harayama, T. *et al.* Lysophospholipid Acyltransferases Mediate Phosphatidylcholine Diversification to Achieve the Physical Properties Required In Vivo. *Cell Metabolism* **20**, 295-305, doi:10.1016/j.cmet.2014.05.019 (2014).

27 Bridges, J. P. *et al.* LPCAT1 regulates surfactant phospholipid synthesis and is required for transitioning to air breathing in mice. *Journal of Clinical Investigation* **120**, 1736-1748, doi:10.1172/jci38061 (2010).

28 Okudaira, M. *et al.* Separation and quantification of 2-acyl-1-lysophospholipids and 1-acyl-2-lysophospholipids in biological samples by LC-MS/MS. *Journal of Lipid Research* **55**, 2178-2192, doi:10.1194/jlr.D048439 (2014).

29 Kawana, H. *et al.* An accurate and versatile method for determining the acyl group-introducing position of lysophospholipid acyltransferases. *Biochim Biophys Acta Mol Cell Biol Lipids* **1864**, 1053-1060, doi:10.1016/j.bbalip.2019.02.008 (2019).

30 Wang, Y. & Li, G. R. TRPC1/TRPC3 channels mediate lysophosphatidylcholine-induced apoptosis in cultured human coronary artery

smooth muscles cells. *Oncotarget* **7**, 50937-50951, doi:10.18632/oncotarget.10853 (2016).

31 Pfeiffer, A. *et al.* Lipopolysaccharide and ceramide docking to CD14 provokes ligand-specific receptor clustering in rafts. *European Journal of Immunology* **31**, 3153-3164, doi:10.1002/1521-4141(200111)31:11<3153::aid-immu3153>3.0.co;2-0 (2001).

32 Triantafilou, M., Miyake, K., Golenbock, D. T. & Triantafilou, K. Mediators of innate immune recognition of bacteria concentrate in lipid rafts and facilitate lipopolysaccharide-induced cell activation. *Journal of Cell Science* **115**, 2603-2611 (2002).

33 Plociennikowska, A., Hromada-Judycka, A., Borzecka, K. & Kwiatkowska, K. Co-operation of TLR4 and raft proteins in LPS-induced pro-inflammatory signaling. *Cellular and Molecular Life Sciences* **72**, 557-581, doi:10.1007/s00018-014-1762-5 (2015).

34 Hancock, J. F. Lipid rafts: contentious only from simplistic standpoints. *Nature Reviews Molecular Cell Biology* **7**, 456-462, doi:10.1038/nrm1925 (2006).

35 Lingwood, D. & Simons, K. Lipid Rafts As a Membrane-Organizing Principle. *Science* **327**, 46-50, doi:10.1126/science.1174621 (2010).

36 Sviridov, D., Mukhamedova, N. & Miller, Y. I. Lipid rafts as a therapeutic target. *Journal of Lipid Research* **61**, 687-695, doi:10.1194/jlr.TR120000658 (2020).

37 Levental, I., Levental, K. R. & Heberle, F. A. Lipid Rafts: Controversies Resolved, Mysteries Remain. *Trends in Cell Biology* **30**, 341-353, doi:10.1016/j.tcb.2020.01.009 (2020).

38 Zhu, X. W. *et al.* Macrophage ABCA1 reduces MyD88-dependent Toll-like

receptor trafficking to lipid rafts by reduction of lipid raft cholesterol. *Journal of Lipid Research* **51**, 3196-3206, doi:10.1194/jlr.M006486 (2010).

39 Field, K. A., Holowka, D. & Baird, B. Fc epsilon RI-mediated recruitment of p53/56lyn to detergent-resistant membrane domains accompanies cellular signaling. *Proc Natl Acad Sci U S A* **92**, 9201-9205, doi:10.1073/pnas.92.20.9201 (1995).

40 Dinic, J., Riehl, A., Adler, J. & Parmryd, I. The T cell receptor resides in ordered plasma membrane nanodomains that aggregate upon patching of the receptor. *Scientific Reports* **5**, doi:10.1038/srep10082 (2015).

41 Gupta, N. & DeFranco, A. L. Visualizing lipid raft dynamics and early signaling events during antigen receptor-mediated B lymphocyte activation. *Faseb Journal* **17**, C203-C203 (2003).

42 Bi, J. F. *et al.* Oncogene Amplification in Growth Factor Signaling Pathways Renders Cancers Dependent on Membrane Lipid Remodeling. *Cell Metabolism* **30**, 525-+, doi:10.1016/j.cmet.2019.06.014 (2019).

43 Blum, J. S., Wearsch, P. A. & Cresswell, P. Pathways of antigen processing. *Annu Rev Immunol* **31**, 443-473, doi:10.1146/annurev-immunol-032712-095910 (2013).

44 Vereb, G. *et al.* Cholesterol-dependent clustering of IL-2Ralpha and its colocalization with HLA and CD48 on T lymphoma cells suggest their functional association with lipid rafts. *Proc Natl Acad Sci U S A* **97**, 6013-6018, doi:10.1073/pnas.97.11.6013 (2000).

45 Hiltbold, E. M., Poloso, N. J. & Roche, P. A. MHC class II-peptide complexes and APC lipid rafts accumulate at the immunological synapse. *Journal of*

Immunology **170**, 1329-1338, doi:10.4049/jimmunol.170.3.1329 (2003).

46 Anderson, H. A. & Roche, P. A. MHC class II association with lipid rafts on the antigen presenting cell surface. *Biochimica Et Biophysica Acta-Molecular Cell Research* **1853**, 775-780, doi:10.1016/j.bbamcr.2014.09.019 (2015).

47 Komaniwa, S. *et al.* Lipid-mediated presentation of MHC class II molecules guides thymocytes to the CD4 lineage. *European Journal of Immunology* **39**, 96-112, doi:10.1002/eji.200838796 (2009).

48 Soupene, E., Fyrst, H. & Kuypers, F. A. Mammalian acyl-CoA : lysophosphatidylcholine acyltransferase enzymes. *Proceedings of the National Academy of Sciences of the United States of America* **105**, 88-93, doi:10.1073/pnas.0709737104 (2008).

49 Drobnik, W. *et al.* Plasma ceramide and lysophosphatidylcholine inversely correlate with mortality in sepsis patients. *Journal of Lipid Research* **44**, 754-761, doi:10.1194/jlr.M200401-JLR200 (2003).

50 Taylor, L. A., Arends, J., Hodina, A. K., Unger, C. & Massing, U. Plasma lyso-phosphatidylcholine concentration is decreased in cancer patients with weight loss and activated inflammatory status. *Lipids in Health and Disease* **6**, doi:10.1186/1476-511x-6-17 (2007).

51 Bligh, E. G. & Dyer, W. J. A RAPID METHOD OF TOTAL LIPID EXTRACTION AND PURIFICATION. *Canadian Journal of Biochemistry and Physiology* **37**, 911-917 (1959).

52 Akagi, S. *et al.* Lysophosphatidylcholine acyltransferase 1 protects against cytotoxicity induced by polyunsaturated fatty acids. *Faseb Journal* **30**, 2027-2039, doi:10.1096/fj.201500149 (2016).

53 Cho, K. W., Morris, D. L. & Lumeng, C. N. Flow Cytometry Analyses of Adipose Tissue Macrophages. *Methods of Adipose Tissue Biology, Pt A* **537**, 297-314, doi:10.1016/b978-0-12-411619-1.00016-1 (2014).

54 Shindou, H. *et al.* Relief from neuropathic pain by blocking of the platelet-activating factor-pain loop. *FASEB J* **31**, 2973-2980, doi:10.1096/fj.201601183R (2017).

55 Wang, H. Y. *et al.* One-Step Generation of Mice Carrying Mutations in Multiple Genes by CRISPR/Cas-Mediated Genome Engineering. *Cell* **153**, 910-918, doi:10.1016/j.cell.2013.04.025 (2013).

Acknowledgement

本研究を進めるにあたり終始ご指導くださった、東京大学大学院 薬学系研究科 衛生化学教室の青木淳賢 教授、河野望 准教授、川名裕己 特任助教、(独) 医療品医療機器総合機構の新井洋由 理事、University of California Los Angeles の嶋中雄太 研究員に心より感謝申し上げます。特に、研究方針に関して日々議論してくださった河野望 准教授、新井洋由 センター長、嶋中雄太 研究員に深く感謝いたします。研究が行き詰まった時、打開するための的確なアドバイスをくださった川名裕己 特任助教に心より感謝いたします。

マウスの供与と研究を進める上で重要な議論をしてくださった、国立国際医療研究センター　脂質シグナリングプロジェクト 進藤英雄 副プロジェクト長、山本将大 研究員に心より感謝申し上げます。

マウスの飼育にあたり、飼育環境を管理し常に支えてくださった、薬学部動物施設 職員の皆様に深く感謝いたします。

研究生活を共にし、本研究を様々な面で支えてくださった衛生化学教室の皆様に心より感謝申し上げます。特に、同期として互いに切磋琢磨した石野雄己 博士、小川笑満里 博士に大変感謝しております。同期の 2 人がいたからこそここまで研究を続けてこられました。また、日々あらゆる面で充実した学生生活・研究環境を整えてくだった、高田祥恵さん、伏間貴子さん、喜安薫さん、大澤由季子さん、道村彩美さん、に心より感謝申し上げます。

火災後、実験スペースや機器を貸してくださった東京大学大学院 薬学系研究科 分子生物学教室の皆様、医学部 RI 施設の管理室の皆様に心より感謝申し上げます。

最後に、私の学生生活を全面的にサポートし応援してくれた、家族に感謝いたします。特に、父 悟、母 トモ子、姉 麻衣、弟 寛也・康平のお蔭で、研究に打ち込むことができ、充実した 3 年間を過ごすことができました。本当にありがとうございました。

令和 4 年 3 月 9 日